Geophys. J. Int. (1993) **114,** 569–592 *and Microfiche GJI* 114/1

Surface potential and gravity changes due to internal dislocations in a spherical earth—I. Theory for a point dislocation

Wenke Sun* and Shuhei Okubo

Earthquake Research Institute, The University of Tokyo, Bunkyo-ku, Tokyo 113, *Japan*

Accepted 1993 February 1. Received 1992 December 14; in original form 1992 July 6

SUMMARY

This paper studies the potential and gravity changes caused by dislocations in spherically symmetric earth models. We define dislocation Love numbers to describe the elastic deformation of the earth raised by point sources. We discuss the shear and tensile dislocations, which can be expressed by four independent components: a vertical strike–slip, a vertical dip–slip, a tensile opening on a horizontal plane, and a tensile opening on a vertical plane.

The results for a homogeneous earth model agree very well, at least within 1°, with those predicted from flat-earth theory. The far-field results indicate no larger than 10 per cent difference within 10°. It makes little difference whether we use the theory on a sphere or that for a flat earth in the near field, while it is reasonable to use the spherical theory for global calculation. We proceed to calculations with a radially heterogeneous earth model (Model 1066A). The results are as a whole similar to those for a homogeneous sphere. In some cases, however, the difference between the two becomes significant. For example, the locations of the nodal lines of the gravity change differ significantly between the two models. This indicates that the vertical layering can cause considerable effects on the deformation fields.

Key words: coseismic change, dislocation, gravity, potential, spherical earth.

1 INTRODUCTION

Since Steketee (1958) introduced dislocation theory to seismology, numerous theoretical formulations have been developed to describe the deformation of an isotropic homogeneous earth model caused by a variety of dislocations. Many scientists (Maruyama 1964; Press 1965; Okada 1985) studied surface displacements, tilt and strain, due to dislocations buried in a semi-infinite medium.

Efforts to develop the formulations in a more realistic earth model have also been advanced through numerous studies (Ben-Menahem & Singh 1968; Ben-Menahem & Israel 1970; Smylie & Mansinha 1971). These studies revealed that the effect of the earth curvature is negligible for shallow events at an epicentral distance less than 20°, while vertical layering or lateral inhomogeneity may have considerable effects on the deformation fields.

Saito (1967) presented a theory to calculate amplitudes of free oscillations caused by a point source in a spherically symmetric earth model. He expressed his results in terms of normal mode solutions and source functions. Kagan (1987a and b) gave the source functions of elementary sources in general form for both static and dynamic displacements.

It was only in the late 1970s when gravity change caused by dislocations was studied by researchers. Hagiwara (1977) first investigated the elevation and gravity changes due to an explosive source. Savage (1984) gave the gravity changes in several special cases: strike–slip faulting on a vertical plane, slip on an infinitely long fault, and so on. Sasai (1986, 1988) studied the surface displacement, gravity and magnetic changes associated with multiple tensile cracks of the Gaussian distribution. Okubo (1991, 1992) completely studied the problem on potential and gravity changes caused by point dislocations and by faulting on a finite plane in a semi-infinite homogeneous medium. He derived all sets of expressions in closed form. They also enable us to evaluate coseismic changes in surface gravity and geoid height.

All of the above studies except Saito (1967) assumed a homogeneous semi-infinite medium or a homogeneous non-gravitating sphere. No one has ever succeeded in computing the displacement, strain, tilt and change in gravity field of a *spherically symmetric and self-gravitating* earth model owing to numerical difficulties.

The objective of this paper is to study global gravity changes caused by dislocations in a spherical earth. We give formulae and numerical results of the radial displacement, potential and gravity changes, due to point dislocations in a spherical earth model. We examine the effects of the spherical curvature and the radial heterogeneity by

*On leave from: Center for Analysis and Prediction of State Seismological Bureau, Beijing, 100036, China.

comparing results for a flat earth, a homogeneous sphere and a radially stratified spherical earth. We may check the consistency between Okubo's (1991) flat-earth theory and our spherical theory.

2 EXCITATION PROBLEM AND RECIPROCITY THEOREM

We discuss two kinds of excitation sources—shear and tensile dislocations. We show that they can be expressed by four independent components: a vertical strike–slip, a vertical dip–slip, an opening of a horizontal crack, and an opening of a vertical crack. We introduce the reciprocity theorem (Okubo 1993) to get our solutions of equations of equilibrium with an arbitrary point dislocation in a SNREI model. We define dislocation Love numbers in Section 2.4.

2.1 Equations of equilibrium for spheroidal deformation

Let us consider a spherically symmetric, non-rotating, perfectly elastic and isotropic, i.e. the SNREI model (Dahlen 1968). For convenience, we assume a point dislocation located on the polar axis at radial distance $r = r_s$; the deformation field due to a source at an arbitrary position can be obtained by simply using the rotational transformation. The geometry of such a dislocation can be uniquely determined by a vector **n** to the infinitesimal fault and by a

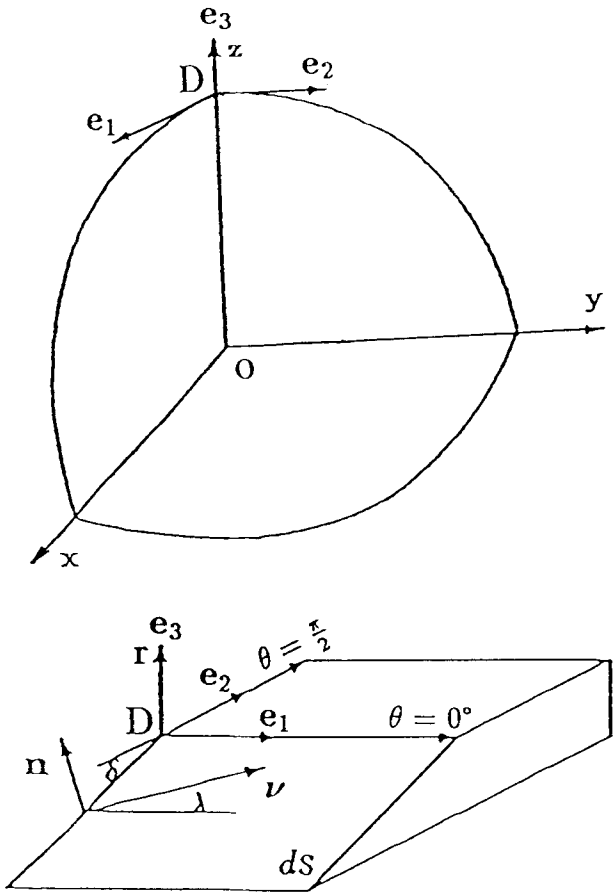

Figure 1. Dislocation model. The upper figure shows the location of an earthquake within a sphere. The lower figure indicates the fault geometry in spherical coordinates.

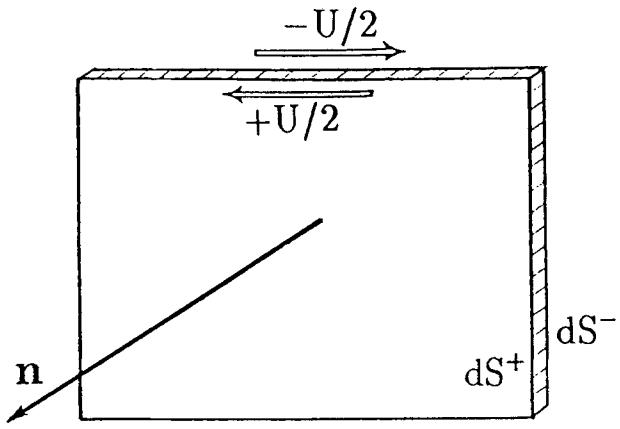

Figure 2. Dislocation U and its normal **n** defined on a fault plane.

Burgers vector $\Delta\mathbf{u}$:

$$\mathbf{n} = n_1\mathbf{e}_1 + n_2\mathbf{e}_2 + n_3\mathbf{e}_3 \tag{1}$$

$$\Delta\mathbf{u} = U \cdot \boldsymbol{\nu} = U(\nu_1\mathbf{e}_1 + \nu_2\mathbf{e}_2 + \nu_3\mathbf{e}_3), \tag{2}$$

where we take unit vectors $\mathbf{e}_1$ and $\mathbf{e}_2$ in the equatorial plane in the direction of $\phi = 0$ and $\pi/2$, respectively, and $\mathbf{e}_3$ along the polar axis (Fig. 1). The sign convention is such that if the sides of an infinitesimal surface dS are labelled dS^- and dS^+, the normal vector **n** points from dS^- to dS^+ and Δu_i is the displacement on dS^+ minus the displacement on dS^- (Fig. 2).

Spheroidal displacement **u**, stress τ, and potential change ψ are conveniently described as

$$\mathbf{u}(r, \theta, \phi) = \sum_{n,m} [y_1(r; n, m)\mathbf{R}_n^m(\theta, \phi) + y_3(r; n, m)\mathbf{S}_n^m(\theta, \phi)] \tag{3}$$

$$\tau \cdot \mathbf{e}_r(r, \theta, \phi) = \sum_{n,m} [y_2(r; n, m)\mathbf{R}_n^m(\theta, \phi) + y_4(r; n, m)\mathbf{S}_n^m(\theta, \phi)] \tag{4}$$

$$\psi(r, \theta, \phi) = \sum_{n,m} y_5(r; n, m)Y_n^m(\theta, \phi) \tag{5}$$

$$\mathbf{R}_n^m(\theta, \phi) = \mathbf{e}_r Y_n^m(\theta, \phi) \tag{6}$$

$$\mathbf{S}_n^m(\theta, \phi) = \left[\mathbf{e}_\theta \frac{\partial}{\partial\theta} + \mathbf{e}_\phi \frac{1}{\sin\theta}\frac{\partial}{\partial\phi}\right] Y_n^m(\theta, \phi) \tag{7}$$

where $\mathbf{e}_r$, $\mathbf{e}_\theta$, $\mathbf{e}_\phi$ are unit vectors in the spherical coordinates, and

$$Y_n^m(\theta, \phi) = P_n^m(\cos\theta)e^{im\phi}. \tag{8}$$

P_n^m is the associated Legendre's function and

$$P_n^{-m}(\cos\theta) = (-1)^m P_n^m(\cos\theta). \tag{9}$$

The linearized first-order equations of equilibrium, stress–strain relation and Poisson's equation for a *spheroidal deformation* can be written as (Saito 1967)

$$\frac{d\mathbf{Y}}{dr} = \mathbf{AY} + \mathbf{S} \tag{10}$$

where $\mathbf{Y} = (y_1, \ldots, y_6)'$, **A** is a matrix coefficient which

depends on density ρ, on the elastic constants λ, μ and on n. In eqs (3)–(10), we strictly follow the notation and formulation by Takeuchi & Saito (1972) which conforms to Alterman, Jarosch & Pekeris (1959) except y_6. A modification has been made for the definition of y_6 as

$$y_6 = \frac{dy_5}{dr} + \frac{n+1}{r} y_5 - 4\pi G\rho y_1. \tag{11}$$

G denotes Newton's gravitational constant. The source function $\mathbf{S}$ is discontinuous across $r = r_s$:

$$\begin{aligned}\mathbf{S} &\equiv (s_1, s_2, \ldots, s_6)\delta(r - r_s)\\ &= [\mathbf{Y}(r_s + 0) - \mathbf{Y}(r_s - 0)]\delta(r - r_s).\end{aligned} \tag{12}$$

Notice that s_5 and s_6 always vanish because the potential ψ and $(\partial\psi/\partial r - 4\pi G\rho u_r)$ must be continuous across any boundary surfaces. The continuity persists even if the radial displacement u_r has a jump at the interface (Saito 1967).

The source functions of spheroidal degree n and order m for the point dislocation are given by Takeuchi & Saito (1972) as

$$s_1(n, m) = \frac{2n+1}{4\pi r_s^2}\left[\nu_3 n_3 + \frac{\lambda}{\lambda + 2\mu}(\nu_1 n_1 + \nu_2 n_2)\right]\delta_{m0} UdS \tag{13}$$

$$s_2(n, m) = -\frac{2n+1}{2\pi r_s^3}\frac{\mu(3\lambda + 2\mu)}{\lambda + 2\mu}(\nu_1 n_1 + \nu_2 n_2)\delta_{m0} UdS \tag{14}$$

$$\begin{aligned}s_3(n, m) = \frac{2n+1}{4\pi n(n+1) r_s^2}\frac{1}{2}&[(\nu_1 n_3 + \nu_3 n_1)(\delta_{m1} - \delta_{m,-1})\\ &- i(\nu_3 n_2 + \nu_2 n_3)\delta_{|m|1}]UdS\end{aligned} \tag{15}$$

$$\begin{aligned}s_4(n, m) = \Bigg\{&\frac{2n+1}{4\pi r_s^3}\frac{\mu(3\lambda + 2\mu)}{\lambda + 2\mu}(\nu_1 n_1 + \nu_2 n_2)\delta_{m0}\\ &+ \frac{2n+1}{4\pi n(n+1) r_s^3}\frac{\mu}{2}\cdot[(-\nu_1 n_1 + \nu_2 n_2)\delta_{|m|2}\\ &+ i(\nu_2 n_1 + \nu_1 n_2)(\delta_{m2} - \delta_{m,-2})]\Bigg\} UdS\end{aligned} \tag{16}$$

$$s_5(n, m) = 0 \tag{17}$$

$$s_6(n, m) = 0 \tag{18}$$

where δ_{ij} is the Kronecker delta. Notice that only the spheroidal orders $|m| \leq 2$ are involved in (13)–(16) because we take the source on the polar axis.

2.2. Four independent solutions

Let Z^{ij} denote either vertical displacement u_r or potential change ψ due to the slip $\Delta\mathbf{u} = \mathbf{e}_i$ on an infinitesimal plane normal to $\mathbf{e}_j$. A deformation field caused by a dislocation $\Delta\mathbf{u}$ on a plane normal to $\mathbf{n}$ is written as

$$Z(r, \theta, \phi) = Z^{ij}(r, \theta, \phi)\nu_i n_j UdS; \qquad i, j = 1, 2, 3 \tag{19}$$

because $\mathbf{S}$ in (10) is expressed in terms of $\nu_i n_j UdS$ [see (13)–(18)]. Z^{ij} is symmetrical with respect to i and j

$$Z^{ji}(r, \theta, \phi) = Z^{ij}(r, \theta, \phi) \tag{20}$$

because $\mathbf{S}$ in (10) is invariant by interchanging i and j [see (13)–(18)]. Hence the number of independent Z^{ij} reduces to six. Furthermore, intrinsic symmetry within the fault geometry indicates that the components Z^{11} and Z^{31} can be easily calculated by applying rotational transformation about the polar axis to Z^{22} and Z^{32}

$$Z^{11}(r, \theta, \phi) = Z^{22}\left(r, \theta, \phi + \frac{\pi}{2}\right) \tag{21}$$

$$Z^{31}(r, \theta, \phi) = Z^{32}\left(r, \theta, \phi + \frac{\pi}{2}\right). \tag{22}$$

Consequently, the number of independent Z^{ij} is 4. In the following, we choose $(Z^{12}, Z^{32}, Z^{22}, Z^{33})$ for the four independent solutions. They are excited by a vertical strike–slip, a vertical dip–slip, a horizontal tensile fracturing, and a vertical tensile fracturing.

2.3 Reciprocity theorem

The basic eq. (10) is inhomogeneous because it includes the $\mathbf{S}$ term which represents a jump at the point source. We must solve the singular inhomogeneous equations with free boundary conditions

$$y_2(a; n, m) = y_4(a; n, m) = y_6(a; n, m) = 0. \tag{23}$$

Smylie & Mansinha (1971) and Takeuchi & Saito (1972) discussed the methods of solving the problem. From a new way here, we solve the problem by introducing Okubo's (1993) reciprocity theorem.

Okubo (1933) found that the deformation on the surface $r = a$ raised by dislocations at $r = r_s$ is expressed simply by that of the tide, load and shear solutions at $r = r_s$. Let superscripts 'Tide', 'Load', and 'Shear' indicate the tide, the load, and the shear solutions respectively (Saito 1978). They are governed by the *homogeneous* differential equation

$$\frac{d\mathbf{Y}}{dr} = \mathbf{A}\mathbf{Y} \tag{24}$$

under appropriate boundary conditions (Table 1). Okubo gave the surface values of the radial functions $\{y_l^{ij}, l = 1, 3, 5\}$ raised by a slip $\Delta\mathbf{u} = \mathbf{e}_i$ on an infinitesimal plane normal to $\mathbf{e}_j$ as follows.

Vertical strike–slip:

$$\begin{aligned}y_1^{12}(a; n, m) = &-\frac{3}{8\pi a^2 \rho_0 \xi}\frac{\mu_s}{r_s}\\ &\times [y_3^{\mathrm{Load}}(r_s; n) - y_3^{\mathrm{Tide}}(r_s; n)]\cdot\delta_{|m|2}\end{aligned} \tag{25}$$

$$y_3^{12}(a; n, m) = \frac{3}{8\pi a^2 \rho_0 \xi}\frac{\mu_s}{r_s} y_3^{\mathrm{Shear}}(r_s; n)\cdot\delta_{|m|2} \tag{26}$$

$$y_5^{12}(a; n, m) = \frac{G g_0 \mu_s}{2 a r_s} y_3^{\mathrm{Tide}}(r_s; n)\cdot\delta_{|m|2}. \tag{27}$$

Table 1. Boundary conditions for tide, load and shear deformations.

	$y_2(a; n, m)$	$y_4(a; n, m)$	$y_6(a; n, m)$
Tide	0	0	$\frac{2n+1}{a}$
Load	$-\frac{(2n+1)g(a)}{4\pi G a}$	0	$\frac{2n+1}{a}$
Shear	0	$\frac{(2n+1)g(a)}{4\pi G a n(n+1)}$	0

Vertical dip-slip:

$$y_1^{32}(a; n, m) = -\frac{3}{8\pi a^2 \rho_0 \xi} \times [y_4^{\text{Load}}(r_s; n) - y_4^{\text{Tide}}(r_s; n)] \cdot \delta_{|m|1} \quad (28)$$

$$y_3^{32}(a; n, m) = \frac{3}{8\pi a^2 \rho_0 \xi} y_4^{\text{Shear}}(r_s; n) \cdot \delta_{|m|1} \quad (29)$$

$$y_5^{32}(a; n, m) = \frac{Gg_0}{2a} y_4^{\text{Tide}}(r_s; n) \cdot \delta_{|m|1}. \quad (30)$$

Horizontal tensile fracturing:

$$y_1^{22}(a; n, m) = -\frac{3}{4\pi a^2 \rho_0 \xi} \left[\frac{\lambda_s}{\sigma_s} [y_2^{\text{Load}}(r_s; n) - y_2^{\text{Tide}}(r_s; n)] + \frac{3k_s}{\sigma_s} \frac{\mu_s}{r_s} \{2[y_1^{\text{Load}}(r_s; n) - y_1^{\text{Tide}}(r_s; n)] - n(n+1)[y_3^{\text{Load}}(r_s; n) - y_3^{\text{Tide}}(r_s; n)]\} \right] \times \delta_{m0} + y_1^{12}(a; n, m) \quad (31)$$

$$y_3^{22}(a; n, m) = \frac{3}{4\pi a^2 \rho_0 \xi} \left\{ \frac{\lambda_s}{\sigma_s} y_2^{\text{Shear}}(r_s; n) + \frac{3K_s}{\sigma_s} \frac{\mu_s}{r_s} \times [2y_1^{\text{Shear}}(r_s; n) - n(n+1) y_3^{\text{Shear}}(r_s; n)] \right\} \times \delta_{m0} + y_3^{12}(a; n, m) \quad (32)$$

$$y_5^{22}(a; n, m) = \frac{Gg_0}{a} \left\{ \frac{\lambda_s}{\sigma_s} y_2^{\text{Tide}}(r_s; n) + \frac{3K_s}{\sigma_s} \frac{\mu_s}{r_s} \times [2y_1^{\text{Tide}}(r_s; n) - n(n+1) y_3^{\text{Tide}}(r_s; n)] \right\} \times \delta_{m0} + y_5^{12}(a; n, m). \quad (33)$$

Vertical tensile fracturing:

$$y_1^{33}(a; n, m) = -\frac{3}{4\pi a^2 \rho_0 \xi} \times [y_2^{\text{Load}}(r_s; n) - y_2^{\text{Tide}}(r_s; n)] \cdot \delta_{m0} \quad (34)$$

$$y_3^{33}(a; n, m) = \frac{3}{4\pi a^2 \rho_0 \xi} y_2^{\text{Shear}}(r_s; n) \cdot \delta_{m0} \quad (35)$$

$$y_5^{33}(a; n, m) = \frac{Gg_0}{a} y_2^{\text{Tide}}(r_s; n) \cdot \delta_{m0}. \quad (36)$$

Here g_0 denotes the gravity on the earth's surface, $\xi = g_0/\gamma a$, $\gamma = \frac{4}{3}\pi G\rho_0$, $\lambda_s = \lambda(r_s)$, $\mu_s = \mu(r_s)$, $\sigma_s = \lambda_s + 2\mu_s$, and $K_s = \lambda_s + \frac{2}{3}\mu_s$. Notice that y_i^{Tide}, y_i^{Load} and y_i^{Shear} are degenerated with respect to the spheroidal order m.

In practice, therefore, we have only to calculate three sets of basic solutions (tide, load and shear) at the point source $r = r_s$ because the coseismic solutions at the earth's surface are given by the above reciprocity theorem. The integration of (10) is thus transformed to the integration of (24). Takeuchi & Saito (1972) and Saito (1974) described in detail how to get the three sets of basic solutions (tide, load and shear).

2.4 Dislocation Love numbers

Love and Shida numbers (we shall collectively call them Love numbers) express the elastic deformation of the earth due to external forces. For example, the tidal Love number triplet (h_n, l_n, k_n) describes the displacement and the gravitational potential change at the surface of the earth. Since a surface mass load also deforms the elastic earth, one can define load Love numbers (h_n', l_n', k_n') (Longman 1962, 1963; Farrell 1972). Saito (1978) defined the shear Love numbers (h_n'', l_n'', k_n'') which specify the elastic response of the earth to a shear force acting on the earth's surface.

In the same way, we define new Love number triplets $[h_{nm}^{ij}, l_{nm}^{ij}, k_{nm}^{ij}]$, so that the spheroidal deformation of the earth raised by a point dislocation is described as

$$\mathbf{u}(a, \theta, \phi) = \frac{1}{a^2} \times \sum_{n,m} [h_{nm}^{ij} \mathbf{R}_n^m(\theta, \phi) + l_{nm}^{ij} \mathbf{S}_n^m(\theta, \phi)] \cdot \nu_i n_j U dS \quad (37)$$

$$\psi(a, \theta, \phi) = \frac{g_0}{a^2} \sum_{n,m} k_{nm}^{ij} Y_n^m(\theta, \phi) \cdot \nu_i n_j U dS. \quad (38)$$

We call $[h_{nm}^{ij}, l_{nm}^{ij}, k_{nm}^{ij}]$ dislocation Love numbers. Comparing eqs (3) (5) with (37) (38), we may derive the relation between the dislocation Love numbers and $\{y_j; j = 1, 2, \ldots, 6\}$ as

$$h_{nm}^{ij} = y_1^{ij}(a; n, m) a^2 \quad (39)$$

$$l_{nm}^{ij} = y_3^{ij}(a; n, m) a^2 \quad (40)$$

$$k_{nm}^{ij} = y_5^{ij}(a; n, m) \frac{a^2}{g_0}. \quad (41)$$

We should notice that the dislocation Love numbers are independent of the magnitude of dislocation UdS. We show the relations between them in Table 2.

When $n = 0$, the dislocation Love numbers l_{00}^{ij} and k_{00}^{ij} are zero because k_{00}^{ij} is proportional to the change in the earth's mass which should be conserved during deformation, and because the spheroidal deformation of degree 0 is free from tangential displacement.

For the special case $n = 1$, Ben-Menahem & Singh (1968) found that the divergence of the term of the degree 1 is due to the fact that a sphere of finite radius cannot remain in static equilibrium under the action of an unbalanced force system. In a load problem, the degree 1 mode of deformation has the similar situation. Farrell (1972) and

Table 2. Relations between dislocation Love numbers and source functions y_k^{ij} in this Table satisfies the source condition $y_k^{ij}(r_s^+) - y_k^{ij}(r_s^-) = s_k$ and free boundary conditions on the earth's surface.

Type	Order	*Source Functions*	*Dislocation Love Numbers*		
Y^{ij}	m	s_k $(k = 1, 2, \cdots, 6)$	$y_1^{ij}(a; n, m)a^2$	$y_3^{ij}(a; n, m)a^2$	$y_5^{ij}(a; n, m)\frac{a^2}{g_0}$
Y^{12}	2	$-\frac{(2n+1)\mu}{8\pi n(n+1)r_s^2}\delta_{k4}$	h_{n2}^{12}	l_{n2}^{12}	k_{n2}^{12}
Y^{32}	1	$\frac{2n+1}{8\pi n(n+1)r_s^2}\delta_{k3}$	h_{n1}^{32}	l_{n1}^{32}	k_{n1}^{32}
Y^{22}	0	$\frac{2n+1}{4\pi r_s^2}\frac{\lambda}{\lambda+2\mu}\delta_{k1}$ $-\frac{2n+1}{2\pi r_s^2}\frac{\mu(3\lambda+2\mu)}{\lambda+2\mu}\delta_{k2}$ $\frac{2n+1}{4\pi r_s^2}\frac{\mu(3\lambda+2\mu)}{\lambda+2\mu}\delta_{k4}$	h_{n0}^{22}	l_{n0}^{22}	k_{n0}^{22}
	2	$\frac{(2n+1)\mu}{8\pi n(n+1)r_s^2}\delta_{k4}$	$-h_{n2}^{12}$	$-l_{n2}^{12}$	$-k_{n2}^{12}$
Y^{33}	0	$\frac{2n+1}{4\pi r_s^2}\delta_{k1}$	h_{n0}^{33}	l_{n0}^{33}	k_{n0}^{33}

Okubo & Endo (1986) studied the problem. They found that the degree 1 mode shifts the centre of the earth, while the centre of mass of the earth plus loading mass should remain fixed with respect to space. In the dislocation problem, there exists the common situation. Computationally, we proceed in the following way.

(1) Obtain two independent solutions to (10): $y_k^{ij;1}(r; 1, m)$ and $y_k^{ij;2}(r; 1, m)$.

(2) Choose the rigid translation $\tilde{y}_k(r; 1, m)$ as the trivial solution to (10):

$$\tilde{y}_1(r; 1, m) = \tilde{y}_3(r; 1, m) = \tilde{y}_5(r; 1, m)/g(r) = 1$$

$$\tilde{y}_2(r; 1, m) = \tilde{y}_4(r; 1, m) = \tilde{y}_6(r; 1, m)/g(r) = 0.$$

(3) Assume a solution: $y_k^{ij}(a; 1, m) = c_1 y_k^{ij;1}(a; 1, m) + c_2 y_k^{ij;2}(a; 1, m) + c_3 y_k(a; 1, m)$.

(4) Find the constants c_1, c_2 and c_3 by using any two of the boundary conditions (23) and a condition $y_5(a; 1, m) = 0$, which is equivalent to choosing the centre of mass of the deformed earth as the origin. Notice that only two are independent in the boundary condition (23) because there automatically holds a consistency relation in the case of $n = 1$ (Farrell 1972; Okubo & Endo 1986):

$$y_2(r; 1, m) + 2y_4(r; 1, m) + g(r)y_6(r; 1, m)/4\pi G = 0.$$

(5) Obtain the degree 1 dislocation Love numbers as

$$h_{1m}^{ij} = y_1^{ij}(a; 1, m)a^2 \tag{42}$$

$$l_{1m}^{ij} = y_3^{ij}(a; 1, m)a^2 \tag{43}$$

$$k_{1m}^{ij} = 0. \tag{44}$$

3 THEORY OF POTENTIAL AND GRAVITY CHANGES

In this section, we focus our attention on potential and gravity changes raised by point dislocations buried in a radially heterogeneous earth model. We first discuss the general theory of potential and gravity changes in Section 3.1. In Sections 3.2–3.5, we show in detail the potential and gravity changes due to vertical strike–slip, vertical dip–slip, horizontal and vertical tensile fracturings. We derive expressions for an arbitrary geometry for practical applications in Sections 3.6–3.7.

3.1 Potential and gravity changes

A dislocation within the earth causes a density change and a displacement of interfaces, perturbing the gravitational potential. The gravitational potential change ψ may be expressed as

$$\psi(r, \theta, \phi) = \psi^{ij}(r, \theta, \phi)\nu_i n_j UdS \tag{45}$$

where ψ^{ij} is the potential change due to a dislocation $\mathbf{\Delta u} = \mathbf{e}_i$ on a plane of infinitesimal area dS with a normal $\mathbf{n} = \mathbf{e}_j$ [see also (19)].

We may expand ψ^{ij} in spherical harmonics as

$$\psi^{ij}(a, \theta, \phi) = \frac{g_0}{a^2}\sum_{n,m} k_{nm}^{ij} Y_n^m(\theta, \phi) \tag{46}$$

where k_{nm}^{ij} can be calculated from (10). Once all the k_{nm}^{ij} for different n and m are given, we have ψ^{ij} and ψ from (46) and (45).

The gravity change at a *space-fixed* point can be calculated from ψ as

$$\Delta g(r, \theta, \phi) = -\frac{\partial \psi}{\partial r}. \tag{47}$$

The gravity change on the earth's surface $r = a$ deserves special attention because we must consider the surface mass distribution $4\pi G\rho u_r$. Across this single layer, the gravity is *not* continuous. The gravity change (positive downward) just *inside* this thin layer is

$$\Delta g_-(a, \theta, \phi) = -\left.\frac{\partial \psi(r, \theta, \phi)}{\partial r}\right|_{r=a-0} = -\sum_{n,m}^{\infty} \left.\frac{dy_5}{dr}\right|_{r=a-0} Y_n^m(\theta, \phi)\nu_i n_j UdS. \tag{48}$$

Since $y_6(a) = 0$, we may substitute

$$\left.\frac{dy_5}{dr}\right|_{r=a-0} = 4\pi G\rho y_1(a) - \frac{n+1}{a} y_5(a) \tag{49}$$

in eq. (48) to obtain

$$\begin{aligned}\Delta g_-(a, \theta, \phi) = &\left[\frac{g_0}{a^3}\sum_{n,m}^{\infty}(n+1)k_{nm}^{ij}Y_n^m(\theta, \phi)\right. \\ &\left. - \frac{4\pi G\rho}{a^2}\cdot\sum_{n,m}^{\infty} h_{nm}^{ij}Y_n^m(\theta, \phi)\right]\nu_i n_j UdS \\ = &\frac{g_0}{a^3}\sum_{n,m}^{\infty}(n+1)k_{nm}^{ij}Y_n^m(\theta, \phi)\nu_i n_j UdS \\ &- 4\pi G\rho u_r(a, \theta, \phi)\end{aligned} \tag{50}$$

where u_r is the radial displacement

$$u_r(a, \theta, \phi) = u_r^{ij}(a, \theta, \phi)\nu_i n_j UdS \tag{51}$$

$$u_r^{ij}(a, \theta, \phi) = \frac{1}{a^2}\sum_{n,m} h_{nm}^{ij}Y_n^m(\theta, \phi). \tag{52}$$

The gravity change $\Delta g_+(a, \theta, \phi)$ just *outside* the single layer is derived from potential theory (Fig. 3) as

$$\Delta g_+ = \Delta g_- + 4\pi G\rho u_r. \tag{53}$$

From now on, we will briefly use $\Delta g(a, \theta, \phi)$ for $\Delta g_+(a + u_r, \theta, \phi)$ because the gravity surveying is usually carried out on the earth's surface.

Substituting (50) into (53), we obtain

$$\Delta g(a, \theta, \phi) = \frac{g_0}{a^3}\sum_{n,m}^{\infty}(n+1)k_{nm}^{ij}Y_n^m(\theta, \phi)\nu_i n_j UdS. \tag{54}$$

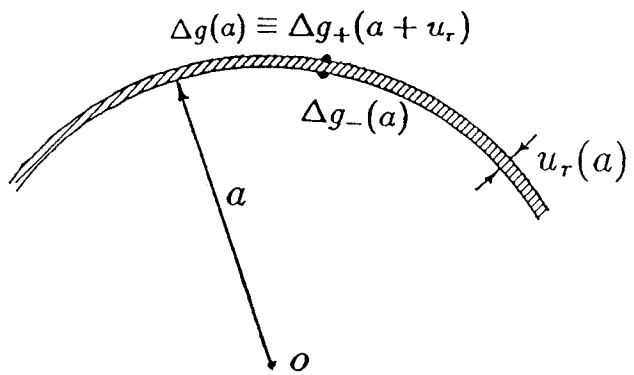

Figure 3. Gravity step on the earth's surface.

The gravity change at a point *fixed on the free surface* becomes

$$\delta g(a, \theta, \phi) = \Delta g(a, \theta, \phi) - \beta u_r(a, \theta, \phi) \tag{55}$$

or

$$\delta g(a, \theta, \phi) = \Delta g_-(a, \theta, \phi) - (\beta - 4\pi G\rho) u_r(a, \theta, \phi) \tag{56}$$

where β is the free-air gravity gradient which can be expressed as

$$\beta = \left| \frac{dg(r)}{dr} \right| = \left| \frac{2g(a)}{a} \right|. \tag{57}$$

3.2 Z^{12}: vertical strike–slip on the polar axis

From this section we are going to derive u_r, ψ, Δg and δg for the four dislocation models assuming dislocation magnitude $UdS = 1$.

We begin with the vertical strike–slip by taking $\mathbf{v} = \mathbf{e}_1$ and $\mathbf{n} = \mathbf{e}_2$. Substituting $\nu_i = \delta_{i1}$ and $n_j = \delta_{j2}$ into (13)–(18), we obtain the source functions

$$s_j^{12}(n, m) = i \frac{(2n+1)\mu}{8\pi n(n+1) r_s^3} \delta_{j4} (\delta_{m2} - \delta_{m,-2}) \tag{58}$$

where the superscript 12 denotes a vertical strike–slip. Hence we obtain the radial displacement u_r^{12} as

$$\begin{aligned} u_r^{12}(r, \theta, \phi) &= -\sum_n i y_1^{12}(r; n, 2) \\ &\quad \times (P_n^2(\cos\theta) e^{2i\phi} - P_n^{-2}(\cos\theta) e^{-2i\phi}) \\ &= 2 \sum_n y_1^{12}(r; n, 2) P_n^2(\cos\theta) \sin 2\phi \end{aligned} \tag{59}$$

where $\{y_j^{12}(r; n, 2);\ j = 1, 2, \ldots, 6\}$ is the excited deformation field with

$$y_j^{12}(r_s^+; n, 2) - y_j^{12}(r_s^-; n, 2) = -\frac{(2n+1)\mu}{8\pi n(n+1) r_s^3} \delta_{j4}, \tag{60}$$

In the same way, we obtain potential change ψ^{12} as

$$\psi^{12}(r, \theta, \phi) = 2 \sum_n y_5^{12}(r; n, 2) P_n^2(\cos\theta) \sin 2\phi. \tag{61}$$

We may further simplify u_r^{12} and ψ^{12} as

$$u_r^{12}(r, \theta, \phi) = \hat{u}_r^{12}(r, \theta) \sin 2\phi \tag{62}$$

$$\psi^{12}(r, \theta, \phi) = \hat{\psi}^{12}(r, \theta) \sin 2\phi \tag{63}$$

by defining

$$\hat{u}_r^{12}(r, \theta) = \frac{2}{a^2} \sum_{n=2}^{\infty} h_{n2}^{12} P_n^2(\cos\theta) \tag{64}$$

$$\hat{\psi}^{12}(r, \theta) = \frac{2g_0}{a^2} \sum_{n=2}^{\infty} k_{n2}^{12} P_n^2(\cos\theta). \tag{65}$$

From (54) and (55) we have gravity changes

$$\Delta g^{12}(a, \theta, \phi) = \Delta \hat{g}^{12}(a, \theta) \sin 2\phi \tag{66}$$

$$\delta g^{12}(a, \theta, \phi) = \delta \hat{g}^{12}(a, \theta) \sin 2\phi \tag{67}$$

where

$$\Delta \hat{g}^{12}(a, \theta) = \frac{2g_0}{a^3} \sum_{n=2}^{\infty} (n+1) k_{n2}^{12} P_n^2(\cos\theta) \tag{68}$$

$$\delta \hat{g}^{12}(a, \theta) = \Delta \hat{g}^{12}(a, \theta) - \beta \hat{u}_r^{12}(a, \theta). \tag{69}$$

Equations (62)–(69) are the fundamental formulae which give the radial displacement, potential and gravity changes at any point (θ, ϕ) at the earth's surface. We present the numerical result of $\hat{u}_r^{12}$, $\hat{\psi}^{12}$, $\Delta \hat{g}^{12}$ and $\delta \hat{g}^{12}$ in Appendix A.

The factor $\sin 2\phi$ in eqs (62), (63), (66) and (67) reveals a quadrant deformation pattern. If u_r (or ψ, Δg, δg) is positive in the quadrants 1 and 3, it becomes negative in the quadrants 2 and 4.

As special cases, let us evaluate the radial displacement, potential and gravity changes for $\theta = 0$ and $\theta = \pi$. Since

$$\lim_{\theta \to 0} Y_n^m(\theta, \phi) = e^{im\phi} \delta_{0m} = \begin{cases} 1; & m = 0 \\ 0; & m \neq 0 \end{cases} \tag{70}$$

and

$$\lim_{\theta \to \pi} Y_n^m(\theta, \phi) = (-1)^n e^{im\phi} \delta_{0m} = \begin{cases} 1; & m = 0, n = \text{odd} \\ -1; & m = 0, n = \text{even} \\ 0; & m \neq 0, \end{cases} \tag{71}$$

it follows that

$$u_r^{12}(a, 0, \phi) = u_r^{12}(a, \pi, \phi) = 0 \tag{72}$$

$$\psi^{12}(a, 0, \phi) = \psi^{12}(a, \pi, \phi) = 0 \tag{73}$$

$$\Delta g^{12}(a, 0, \phi) = \Delta g^{12}(a, \pi, \phi) = 0 \tag{74}$$

$$\delta g^{12}(a, 0, \phi) = \delta g^{12}(a, \pi, \phi) = 0. \tag{75}$$

3.3 Z^{32}: vertical dip–slip on the polar axis

In this section, we derive the potential and gravity changes caused by a vertical dip–slip by assuming $\mathbf{v} = \mathbf{e}_3$, $\mathbf{n} = \mathbf{e}_2$ and $UdS = 1$.

Substituting $\nu_i = \delta_{i3}$ and $n_j = \delta_{j2}$ into (13)–(18), the source functions become

$$s_j^{32}(n, m) = -i \frac{2n+1}{8\pi n(n+1) r_s^2} \delta_{j3} \delta_{|m|1} \tag{76}$$

where the superscript 32 denotes a vertical dip–slip. We obtain the radial displacement u_r^{32} as

$$\begin{aligned} u_r^{32}(a, \theta, \phi) &= -\sum_n i y_1^{32}(a; n, 1) [P_n^1(\cos\theta) e^{i\phi} + P_n^{-1}(\cos\theta) e^{-i\phi}] \\ &= 2 \sum_n y_1^{32}(a; n, 1) P_n^1(\cos\theta) \sin\phi \end{aligned} \tag{77}$$

where $\{y_j^{32}(r; n, 1);\ j = 1, 2, \ldots, 6\}$ is a real-valued solution defined by

$$y_j^{32}(r_s^+; n, 1) - y_j^{32}(r_s^{-1}; n, 1) = \frac{2n+1}{8\pi n(n+1) r_s^2} \delta_{j3}. \tag{78}$$

We may simplify (77) as

$$u_r^{32}(a, \theta, \phi) = \hat{u}_r^{32}(a, \theta) \sin\phi \tag{79}$$

$$\hat{u}_r^{32}(a, \theta) = \frac{2}{a^2} \sum_{n=1}^{\infty} h_{n1}^{32} P_n^1(\cos\theta). \tag{80}$$

Similarly, we obtain the potential and gravity changes on the earth's surface $r = a$ due to a vertical dip–slip dislocation

as

$$\psi^{32}(a, \theta, \phi) = \hat{\psi}^{32}(a, \theta) \sin \phi \tag{81}$$

$$\Delta g^{32}(a, \theta, \phi) = \Delta \hat{g}^{32}(a, \theta) \sin \phi \tag{82}$$

$$\delta g^{32}(a, \theta, \phi) = \delta \hat{g}^{32}(a, \theta) \sin \phi, \tag{83}$$

where

$$\hat{\psi}^{32}(a, \theta) = \frac{2g_0}{a^2} \sum_{n=1}^{\infty} k_{n1}^{32} P_n^1(\cos \theta) \tag{84}$$

$$\Delta \hat{g}^{32}(a, \theta) = \frac{2g_0}{a^3} \sum_{n=1}^{\infty} (n+1) k_{n1}^{32} P_n^1(\cos \theta) \tag{85}$$

$$\delta \hat{g}^{32}(a, \theta) = \Delta \hat{g}^{32}(a, \theta) - \beta \hat{u}_r^{32}(a, \theta). \tag{86}$$

The factor $\sin \phi$ in (79)–(83) reveals that the deformation pattern is anti-symmetric with respect to the fault line defined by $\phi = 0$ and $\phi = \pi$.
$\hat{u}_r^{32}$, $\hat{\psi}^{32}$, $\Delta \hat{g}^{32}$ and $\delta \hat{g}^{32}$ vanish on the two poles ($\theta = 0, \pi$) because P_n^1 in eqs (80)–(86) is proportional to $\sin \theta$.

3.4 Z^{22}: tensile fracturing on a vertical plane

Now we study the potential and gravity changes raised by a tensile dislocation $\Delta \mathbf{u} = \mathbf{e}_2$ on a vertical plane normal to $\mathbf{n} = \mathbf{e}_2$ assuming $UdS = 1$.

Substituting $\nu_i = n_i = \delta_{i2}$ into (13)–(18), the source functions are non-zero only when $m = 0$ and $|m| = 2$. It follows that

$$u_r^{22}(a, \theta, \phi) = u_r^{22,0}(a, \theta, \phi) + u_r^{22,2}(a, \theta, \phi) \tag{87}$$

$$\psi^{22}(a, \theta, \phi) = \psi^{22,0}(a, \theta, \phi) + \psi^{22,2}(a, \theta, \phi) \tag{88}$$

$$\Delta g^{22}(a, \theta, \phi) = \Delta g^{22,0}(a, \theta, \phi) + \Delta g^{22,2}(a, \theta, \phi) \tag{89}$$

$$\delta g^{22}(a, \theta, \phi) = \delta g^{22,0}(a, \theta, \phi) + \delta g^{22,2}(a, \theta, \phi). \tag{90}$$

When $m = 0$, the source functions are

$$s_j^{22}(n, 0) = \frac{2n+1}{4\pi r_s^2} \frac{\lambda}{\lambda + 2\mu} \delta_{j1} - \frac{2n+1}{2\pi r_s^3} \frac{\mu(3\lambda + 2\mu)}{\lambda + 2\mu} \delta_{j2} + \frac{2n+1}{4\pi r_s^3} \frac{\mu(3\lambda + 2\mu)}{\lambda + 2\mu} \delta_{j4}. \tag{91}$$

Since the excited field of order $m = 0$ is independent of ϕ, we have

$$u_r^{22,0}(a, \theta, \phi) = \hat{u}_r^{22,0}(a, \theta) = \frac{1}{a^2} \sum_{n=0}^{\infty} h_{n0}^{22} P_n(\cos \theta) \tag{92}$$

$$\psi^{22,0}(a, \theta, \phi) = \hat{\psi}^{22,0}(a, \theta) = \frac{g_0}{a^2} \sum_{n=0}^{\infty} k_{n0}^{22} P_n(\cos \theta) \tag{93}$$

$$\Delta g^{22,0}(a, \theta, \phi) = \Delta \hat{g}^{22,0}(a, \theta) = \frac{g_0}{a^3} \sum_{n=0}^{\infty} (n+1) k_{n0}^{22} P_n(\cos \theta) \tag{94}$$

$$\delta g^{22,0}(a, \theta, \phi) = \delta \hat{g}^{22,0}(a, \theta) = \Delta \hat{g}^{22,0}(a, \theta) - \beta \hat{u}_r^{22,0}(a, \theta) \tag{95}$$

where h_{n0}^{22}, l_{n0}^{22} and k_{n0}^{22} are the dislocation Love numbers. Since (92)–(95) are independent of longitude ϕ, the earth's surface deforms with a pattern of concentric circles about the north pole.

When $|m| = 2$, the source functions are

$$s_j^{22}(n, m) = \frac{(2n+1)\mu}{8\pi n(n+1) r_s^3} \delta_{j4} \delta_{|m|2} \tag{96}$$

Comparing them with (58) for the vertical strike–slip model leads to the following relationship

$$s_j^{22}(n, \pm 2) = \mp i s_j^{12}(n, \pm 2). \tag{97}$$

(97) implies $u_r^{22,2}$ excited by the $s_j^{22}(n, \pm 2)$ can be written as

$$u_r^{22,2}(a, \theta, \phi) = -\sum_n y_l^{12}(a; n, 2) \times [P_n^2(\cos \theta) e^{2i\phi} + P_n^{-2}(\cos \theta) e^{-2i\phi}] \tag{98}$$

or equivalently as

$$u_r^{22,2}(a, \theta, \phi) = -\hat{u}_r^{12}(a, \theta) \cos 2\phi \tag{99}$$

where $\hat{u}_r^{12}$ is already given in Section 3.2.

Similarly we have

$$\psi^{22,2}(a, \theta, \phi) = -\hat{\psi}^{12}(a, \theta) \cos 2\phi \tag{100}$$

$$\Delta g^{22,2}(a, \theta, \phi) = -\Delta \hat{g}^{12}(a, \theta) \cos 2\phi \tag{101}$$

$$\delta g^{22,2}(a, \theta, \phi) = -\delta \hat{g}^{12}(a, \theta) \cos 2\phi. \tag{102}$$

In summary, we have

$$u_r^{22}(a, \theta, \phi) = \hat{u}_r^{22,0}(a, \theta) - \hat{u}_r^{12}(a, \theta) \cos 2\phi \tag{103}$$

$$\psi^{22}(a, \theta, \phi) = \hat{\psi}^{22,0}(a, \theta) - \hat{\psi}^{12}(a, \theta) \cos 2\phi \tag{104}$$

$$\Delta g^{22}(a, \theta, \phi) = \Delta \hat{g}^{22,0}(a, \theta) - \Delta \hat{g}^{12}(a, \theta) \cos 2\phi \tag{105}$$

$$\delta g^{22}(a, \theta, \phi) = \delta \hat{g}^{22,0}(a, \theta) - \delta \hat{g}^{12}(a, \theta) \cos 2\phi. \tag{106}$$

3.5 Z^{33}: tensile fracturing on a horizontal plane

We consider tensile fracturing on a horizontal plane by taking $\mathbf{v} = \mathbf{e}_3$, $\mathbf{n} = \mathbf{e}_3$ and $UdS = 1$. Substituting $\nu_i = \delta_{i3}$ and $n_j = \delta_{j3}$ into (13)–(18), we obtain the source functions as

$$s_j^{33}(n, m) = \frac{2n+1}{4\pi r_s^2} \delta_{j1} \delta_{m0}. \tag{107}$$

The deformation caused by the tensile dislocation of unit magnitude ($UdS = 1$) is obtained as

$$u_r^{33}(a, \theta, \phi) = \hat{u}_r^{33}(a, \theta) = \frac{1}{a^2} \sum_{n=0}^{\infty} h_{n0}^{33} P_n(\cos \theta) \tag{108}$$

$$\psi^{33}(a, \theta, \phi) = \hat{\psi}^{33}(a, \theta) = \frac{g_0}{a^2} \sum_{n=0}^{\infty} k_{n0}^{33} P_n(\cos \theta) \tag{109}$$

$$\Delta g^{33}(a, \theta, \phi) = \Delta \hat{g}^{33}(a, \theta) = \frac{g_0}{a^3} \sum_{n=0}^{\infty} (n+1) k_{n0}^{33} P_n(\cos \theta) \tag{110}$$

$$\delta g^{33}(a, \theta, \phi) = \delta \hat{g}^{33}(a, \theta) = \Delta \hat{g}^{33}(a, \theta) - \beta \hat{u}_r^{33}(a, \theta) \tag{111}$$

where h_{n0}^{33}, l_{n0}^{33} and k_{n0}^{33} are the dislocation Love numbers excited by (107).

Equations (108)–(111) indicate that the earth's surface deforms with a pattern of concentric circles about the north pole because they are independent of longitude ϕ.

Numerical results of $\hat{u}_r^{ij}$, $\hat{\psi}^{ij}$, $\Delta \hat{g}^{ij}$ and $\delta \hat{g}^{ij}$ are given in Appendix A.

3.6 Inclined dislocation on the polar axis

We consider an inclined dislocation on the polar axis. Furthermore, we assume the fault line is in the direction of $\phi = 0$ (Greenwich meridian).

3.6.1 Shear dislocation

A dislocation vector $\mathbf{v}$ and its normal $\mathbf{n}$ can be expressed in terms of dip-angle δ, and slip-angle λ of the fault (Fig. 1) as

$$\mathbf{n} = \mathbf{e}_3 \cos\delta - \mathbf{e}_2 \sin\delta \tag{112}$$

$$\mathbf{v} = \mathbf{e}_3 \sin\delta \sin\lambda + \mathbf{e}_1 \cos\lambda + \mathbf{e}_2 \cos\delta \sin\lambda. \tag{113}$$

If the dislocation vector $\mathbf{v}$ runs parallel to the fault plane, we have a shear dislocation problem.

Let $Z^{(s)}$ denote $\{u_r, \psi, \Delta g, \delta g\}$ excited by a shear dislocation of unit magnitude $UdS = 1$. From (19)–(22), we have

$$\begin{aligned} Z^{(s)}(a, \theta, \phi) &= Z^{ij}(a, \theta, \phi) v_i n_j \\ &= \cos\lambda[-Z^{12}\sin\delta + Z^{13}\cos\delta] \\ &\quad + \sin\lambda[\tfrac{1}{2}(Z^{33} - Z^{22})\sin 2\delta + Z^{32}\cos 2\delta] \end{aligned} \tag{114}$$

where

$$Z^{13}(a, \theta, \phi) = Z^{32}\left(a, \theta, \phi + \frac{\pi}{2}\right). \tag{115}$$

3.6.2 Tensile dislocation

We consider a tensile dislocation problem by taking

$$\mathbf{v} = \mathbf{n} = \mathbf{e}_3 \cos\delta - \mathbf{e}_2 \sin\delta. \tag{116}$$

Let $Z^{(t)}$ denote $\{u_r, \psi, \Delta g, \delta g\}$ excited by a tensile dislocation of $UdS = 1$. It follows from (19)–(22)

$$\begin{aligned} Z^{(t)}(a, \theta, \phi) &= Z^{ij}(a, \theta, \phi) v_i n_j \\ &= Z^{33}(a, \theta, \phi)\cos^2\delta + Z^{22}(a, \theta, \phi)\sin^2\delta \\ &\quad - Z^{32}(a, \theta, \phi)\sin 2\delta. \end{aligned} \tag{117}$$

3.7 Point dislocation at an arbitrary point

In practice, the dislocation is not necessarily on the polar axis nor the fault line is along the Greenwich meridian. In the following, we derive formulae for an inclined dislocation at an arbitrary point.

Let the point dislocation and the observation station be at $D(\theta_1, \phi_1)$ and $P(\theta_2, \phi_2)$ (Fig. 4). The angular distance between $D(\theta_1, \phi_1)$ and $P(\theta_2, \phi_2)$ is denoted by φ. The fault plane is defined by its strike azimuth z_1 on the earth's surface, measured here clockwise from north. The azimuth of P with respect to the point $D(\theta_1, \phi_1)$ is denoted as z_2 (clockwise from north). We define z as the azimuth of the calculating point with respect to the fault line

$$z = z_1 - z_2 \tag{118}$$

φ and z_2 are derived from spherical trigonometric formulae as

$$\cos\varphi = \cos\theta_1 \cos\theta_2 + \sin\theta_1 \sin\theta_2 \cos(\phi_2 - \phi_1) \tag{119}$$

$$\sin z_2 = \frac{1}{\sin\varphi} \sin\theta_2 \sin(\phi_2 - \phi_1) \tag{120}$$

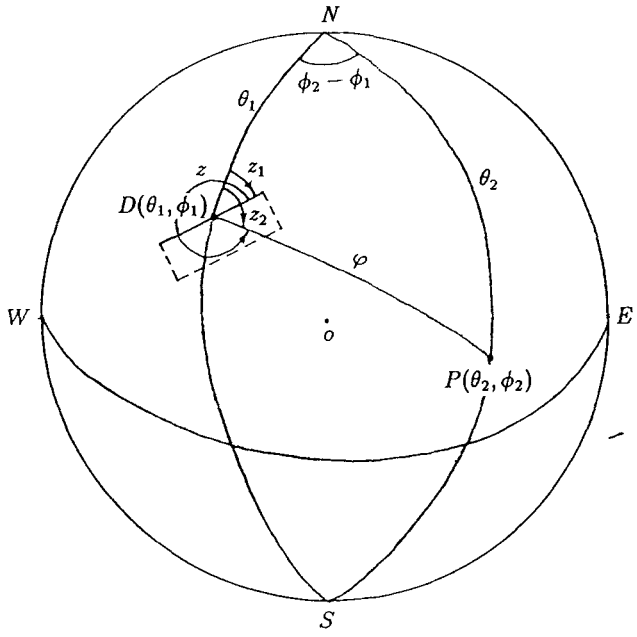

Figure 4. Geometry of a dislocation D and the observation point P.

$$\cos z_2 = \frac{1}{\sin\theta_1 \sin\varphi}(\cos\theta_2 - \cos\theta_1 \cos\varphi). \tag{121}$$

Therefore, we have the following formulae.

Shear dislocation with arbitrary dip and slip angles δ, λ [from (114)]

$$\begin{aligned} u_r^{(s)}(a, \varphi, z) &= \cos\lambda[-\hat{u}_r^{12}(a, \varphi)\sin\delta\sin 2z \\ &\quad + \hat{u}_r^{32}(a, \varphi)\cos\delta\cos z] + \sin\lambda \\ &\quad \times\{\tfrac{1}{2}\sin 2\delta[\hat{u}_r^{33}(a, \varphi) - \hat{u}_r^{22,0}(a, \varphi) \\ &\quad + \hat{u}_r^{12}(a, \varphi)\cos 2z] + \hat{u}_r^{32}(a, \varphi)\cos 2\delta \sin z\} \end{aligned} \tag{122}$$

$$\begin{aligned} \psi^{(s)}(a, \varphi, z) &= \cos\lambda[-\hat{\psi}^{12}(a, \varphi)\sin\delta\sin 2z \\ &\quad + \hat{\psi}^{32}(a, \varphi)\cos\delta\cos z] + \sin\lambda \\ &\quad \times\{\tfrac{1}{2}\sin 2\delta[\hat{\psi}^{33}(a, \varphi) - \hat{\psi}^{22,0}(a, \varphi) \\ &\quad + \hat{\psi}^{12}(a, \varphi)\cos 2z] + \hat{\psi}^{32}(a, \varphi)\cos 2\delta \sin z\} \end{aligned} \tag{123}$$

$$\begin{aligned} \Delta g^{(s)}(a, \varphi, z) &= \cos\lambda[-\Delta\hat{g}^{12}(a, \varphi)\sin\delta\sin 2z \\ &\quad + \Delta\hat{g}^{32}(a, \varphi)\cos\delta\cos z] + \sin\lambda \\ &\quad \times\{\tfrac{1}{2}\sin 2\delta[\Delta\hat{g}^{33}(a, \varphi) - \Delta\hat{g}^{22,0}(a, \varphi) \\ &\quad + \Delta\hat{g}^{12}(a, \varphi)\cos 2z] + \Delta\hat{g}^{32}(a, \varphi) \\ &\quad \times\cos 2\delta \sin z\} \end{aligned} \tag{124}$$

$$\begin{aligned} \delta g^{(s)}(a, \varphi, z) &= \cos\lambda[-\delta\hat{g}^{12}(a, \varphi)\sin\delta\sin 2z \\ &\quad + \delta\hat{g}^{32}(a, \varphi)\cos\delta\cos z] + \sin\lambda \\ &\quad \times\{\tfrac{1}{2}\sin 2\delta[\delta\hat{g}^{33}(a, \varphi) - \delta\hat{g}^{22,0}(a, \varphi) \\ &\quad + \delta\hat{g}^{12}(a, \varphi)\cos 2z] + \delta\hat{g}^{32}(a, \varphi) \\ &\quad \times\cos 2\delta \sin z\}. \end{aligned} \tag{125}$$

Tensile dislocation with an arbitrary dip-angle δ [from 117)]:

$$u_r^{(t)}(a,\varphi,z) = \hat{u}_r^{33}(a,\varphi)\cos^2\delta + [u_r^{22,0}(a,\varphi) - \hat{u}_r^{12}(a,\varphi)\cos 2z]\sin^2\delta - \hat{u}_r^{32}(a,\varphi)\sin 2\delta \sin z \quad (126)$$

$$\psi^{(t)}(a,\varphi,z) = \hat{\psi}^{33}(a,\varphi)\cos^2\delta + [\hat{\psi}^{22,0}(a,\varphi) - \hat{\psi}^{12}(a,\varphi)\cos 2z]\sin^2\delta - \hat{\psi}^{32}(a,\varphi)\sin 2\delta \sin z \quad (127)$$

$$\Delta g^{(t)}(a,\varphi,z) = \Delta\hat{g}^{33}(a,\varphi)\cos^2\delta + [\Delta\hat{g}^{22,0}(a,\varphi) - \Delta\hat{g}^{12}(a,\varphi)\cos 2z]\sin^2\delta - \Delta\hat{g}^{32}(a,\varphi)\sin 2\delta \sin z \quad (128)$$

$$\delta g^{(t)}(a,\varphi,z) = \delta\hat{g}^{33}(a,\varphi)\cos^2\delta + [\delta\hat{g}^{22,0}(a,\varphi) - \delta\hat{g}^{12}(a,\varphi)\cos 2z]\sin^2\delta - \delta\hat{g}^{32}(a,\varphi)\sin 2\delta \sin z. \quad (129)$$

In summary, we may obtain the deformation on the surface by taking the following procedure.

(1) Compute epicentral distance φ and azimuth z of the observation point $P(\theta_2, \phi_2)$ from the dislocation at $D(\theta_1, \phi_1)$ after (119)–(121).

(2) Compute $\hat{u}_r^{ij}(a,\varphi)$, $\hat{\psi}^{ij}(a,\varphi)$, $\Delta\hat{g}^{ij}(a,\varphi)$ and $\delta\hat{g}^{ij}(a,\varphi)$ as described in Sections (3.2)–(3.5) (or from the Tables A.1–A.16).

(3) Use formulae (122) through (129) to compute $u_r^T(a,\varphi,z)$, $\psi^T(a,\varphi,z)$, $\Delta g^T(a,\varphi,z)$ and $\delta g^T(a,\varphi,z)$. These deformation fields are due to a point dislocation of unit magnitude $UdS = 1$.

(4) Reverse the results of (3) back to get their actual units (since we have made some normalizations in Tables A1–A16). With considering UdS, the final results are

$$u_r(a,\varphi,z) = u_r^T(a,\varphi,z)\frac{UdS}{a^2} \quad (130)$$

$$\psi(a,\varphi,z) = \psi^T(a,\varphi,z)\frac{g_0 UdS}{a^2} \quad (131)$$

$$\Delta g(a,\varphi,z) = \Delta g^T(a,\varphi,z)\frac{g_0 UdS}{a^3} \quad (132)$$

$$\delta g(a,\varphi,z) = \delta g^T(a,\varphi,z)\frac{g_0 UdS}{a^3}. \quad (133)$$

4 COMPUTATIONAL TECHNIQUES

4.1 Truncation of the infinite series

Since it is impossible to calculate the dislocation Love numbers to infinite degrees, we must truncate the series such as

$$\frac{1}{a^2}\sum_{n,m}^{\infty} h_{nm}^{ij} P_n(\cos\theta) \simeq \frac{1}{a^2}\sum_{n}^{N}\sum_{m=-2}^{2} h_{nm}^{ij} P_n(\cos\theta) \quad (134)$$

where N is the truncation order. In the following, we discuss the appropriate choice of N.

Okubo's (1988) asymptotic solutions imply that all the Love numbers are proportional to $(r_s/a)^n$:

$$(h_n, l_n, k_n) \propto \left(\frac{r_s}{a}\right)^n \quad (135)$$

where $r_s = a - d_s$ is the radial distance of the point source. Eq. (135) indicates that the deeper the point source, the faster the series (134) converges with n.

Since

$$\left(\frac{r_s}{a}\right)^n = e^{-n\cdot d_s/a}\cdot\left[1 + 0\left(\frac{1}{n}\right)\right], \quad (136)$$

the truncated series $\sum_{n=0}^{N} h_{nm}^{ij} P_n(\cos\theta)$ gives a sufficiently accurate result if

$$e^{-N\cdot d_s/a} \ll 1 \quad \text{or} \quad N \gg \frac{a}{d_s}. \quad (137)$$

We take

$$N \sim 10\frac{a}{d_s} \quad (138)$$

since $(r_s/a)^N \sim e^{-10}$ guarantees the accuracy of 10^{-5}. Notice that N becomes very large ($N \geq 50\,000$) when $d_s < 1$ km.

4.2 Disc factor

To accelerate the convergence of the infinite series as

$$\hat{u}_r^{12}(r,\theta) = \frac{2}{a^2}\sum_{n=2}^{\infty} h_{n2}^{12} P_n^2(\cos\theta), \quad (139)$$

we multiply the summand by a disc factor D_n

$$D_n = -\frac{1+\cos\alpha}{n(n+1)\sin\alpha}\frac{\partial P_n(\cos\alpha)}{\partial\alpha}. \quad (140)$$

Since

$$\lim_{\alpha\to 0} D_n \to \frac{2J_1(n\alpha)}{n\alpha} \to 1 \quad \text{for } n \gg 1, \quad (141)$$

we may rewrite (139) as

$$\hat{u}_r^{12}(r,\theta) = \frac{2}{a^2}\lim_{\alpha\to 0}\sum_{n=2}^{\infty} h_{n2}^{12} D_n P_n^2(\cos\theta). \quad (142)$$

$\hat{u}_r^{12}$ is accurately evaluated by $2/a^2\sum_{n=2}^{\infty} h_{n2}^{12} D_n P_n^2$ when $\theta/\alpha > 10$. The disc factor has a physical meaning of a disc load (Farrell 1972). Let γ be a unit mass distributed uniformly over a disc of radius α,

$$\gamma(\theta;\alpha) = \frac{1}{\pi\alpha^2}; \quad \text{for } \theta \leq \alpha \quad (143)$$

$$= 0; \quad \text{for } \theta > \alpha. \quad (144)$$

Expanding γ in a Legendre series gives

$$\gamma(\theta;\alpha) = \sum_{n=0}^{\infty}\frac{2n+1}{4\pi a^2} D_n P_n(\cos\theta). \quad (145)$$

4.3 Euler transformation

The Euler transformation is a method for evaluating an alternating series. The theory of the Euler transformation states that, if an alternating series $\sum_{n=0}^{\infty}(-1)^n x_n (x_n \geq 0)$ converges, it can be transformed to

$$\sum_{n=0}^{\infty}(-1)^n x_n = \tfrac{1}{2}\sum_{n=0}^{\infty}(-\tfrac{1}{2})^n \Delta^n x_0 \quad (146)$$

where Δ^n is nth order difference of x_n. The Euler transformation accelerates the convergence of many series.

We must transform an original series into an alternating one in advance before applying the Euler transformation. For example, consider a radial displacement with including the disc factor

$$u_r = \frac{1}{a^2}\sum_{n=0}^{\infty} h^{ij}_{nm} D_n P_n(\cos\theta). \tag{147}$$

The Euler transformation cannot be immediately applied to (148) since it is not an alternating series.

We have to transform (148) to partial series

$$u_r = \underbrace{\frac{1}{a^2}\sum_{n=0}^{n_1-1} h^{ij}_{nm} D_n P_n}_{x_0>0} + \underbrace{\frac{1}{a^2}\sum_{n=n_1}^{n_2-1} h^{ij}_{nm} D_n P_n}_{x_1<0} + \underbrace{\frac{1}{a^2}\sum_{n=n_2}^{n_3-1} h^{ij}_{nm} D_n P_n}_{x_2>0} + \cdots \tag{148}$$

or

$$u_r = \sum_{j=0}^{\infty} (-1)^j |x_j|,$$

so that the Euler transformation may be applied to (149).

4.4 Interpolation

The dislocation Love numbers $[h^{ij}_{nm}, l^{ij}_{nm}, k^{ij}_{nm}]$ must be known over a large range of spheroidal degree n. It is not necessary to integrate numerically the equations of equilibrium for each n if interpolation on a sparser table could give accurate dislocation Love numbers. A naïve interpolation method, however, will bring large error because dislocation Love numbers vary rapidly with n (e.g. Table 3). For example, the l^{12}_{n2} in Table 3 varies from 10^1 to 10^{-9} over $2 \le n \le 2000$.

Table 3. Dislocation Love numbers of a homogeneous earth model. Vertical strike–slip fault. $\delta = 90°$, $\lambda = 0°$, $m = 2$. Source depth = 32 km.

n	h^{12}_{n2}	l^{12}_{n2}	k^{12}_{n2}
2	.1316E − 2	.1368E − 1	.2352E − 2
3	−.2030E − 2	.5764E − 2	.6586E − 3
4	−.2270E − 2	.3228E − 2	.2876E − 3
5	−.2100E − 2	.2065E − 2	.1558E − 3
6	−.1877E − 2	.1432E − 2	.9632E − 4
8	−.1491E − 2	.8003E − 3	.4700E − 4
10	−.1207E − 2	.5071E − 3	.2808E − 4
15	−.7760E − 3	.2180E − 3	.1225E − 4
20	−.5409E − 3	.1180E − 3	.7391E − 5
30	−.2969E − 3	.4826E − 4	.3965E − 5
40	−.1747E − 3	.2487E − 4	.2648E − 5
50	−.1035E − 3	.1454E − 4	.1952E − 5
70	−.2780E − 4	.6146E − 5	.1226E − 5
100	.1915E − 4	.2230E − 5	.7278E − 6
200	.4234E − 4	.1540E − 6	.2180E − 6
300	.3185E − 4	−.7950E − 8	.8777E − 7
500	.1348E − 4	−.1403E − 7	.1924E − 7
700	.5212E − 5	−.5038E − 8	.5022E − 8
1000	.1199E − 5	−.9384E − 9	.7765E − 9
1200	.4449E − 6	−.3046E − 9	.2364E − 9
1400	.1643E − 6	−.9963E − 10	.7405E − 10
1600	.6054E − 7	−.3286E − 10	.2368E − 10
1800	.2225E − 7	−.1093E − 10	.7690E − 11
2000	.8172E − 8	−.3662E − 11	.2529E − 11

Table 4. Transformed dislocation Love numbers. Homogeneous earth model with a vertical strike–slip fault. $\delta = 90°$, $\lambda = 0°$, $m = 2$. Source depth = 32 km.

n	$h^{12}_{n2}(\frac{a}{d_s})^n$	$l^{12}_{n2}n(\frac{a}{r_s})^n$	$k^{12}_{n2}n(\frac{a}{r_s})^n$
2	.1329E − 2	.2763E − 1	.4751E − 2
3	−.2061E − 2	.1755E − 1	.2006E − 2
4	−.2316E − 2	.1317E − 1	.1174E − 2
5	−.2154E − 2	.1059E − 1	.7990E − 3
6	−.1935E − 2	.8856E − 2	.5957E − 3
8	−.1552E − 2	.6666E − 2	.3915E − 3
10	−.1270E − 2	.5333E − 2	.2953E − 3
15	−.8369E − 3	.3527E − 2	.1982E − 3
20	−.5982E − 3	.2610E − 2	.1635E − 3
30	−.3453E − 3	.1684E − 2	.1384E − 3
40	−.2137E − 3	.1217E − 2	.1296E − 3
50	−.1331E − 3	.9350E − 3	.1255E − 3
70	−.3955E − 4	.6120E − 3	.1221E − 3
100	.3168E − 4	.3689E − 3	.1204E − 3
200	.1159E − 3	.8431E − 4	.1194E − 3
300	.1443E − 3	−.1080E − 4	.1193E − 3
500	.1671E − 3	−.8701E − 4	.1193E − 3
700	.1769E − 3	−.1197E − 3	.1193E − 3
1000	.1844E − 3	−.1443E − 3	.1194E − 3
1200	.1873E − 3	−.1539E − 3	.1194E − 3
1400	.1894E − 3	−.1607E − 3	.1195E − 3
1600	.1910E − 3	−.1659E − 3	.1195E − 3
1800	.1922E − 3	−.1699E − 3	.1195E − 3
2000	.1932E − 3	−.1731E − 3	.1196E − 3

It is known from Okubo's asymptotic solutions that all Love numbers are appropriately scaled by a factor $(a/r_s)^n$. Hence, we multiply the dislocation Love numbers by $(a/r_s)^n$ to make them vary gently with n as

$$\bar{h}^{ij}_{nm} = h^{ij}_{nm} n^{m-2}\left(\frac{a}{r_s}\right)^n \tag{150}$$

$$\bar{l}^{ij}_{nm} = l^{ij}_{nm} n^{m-1}\left(\frac{a}{r_s}\right)^n \tag{151}$$

$$\bar{k}^{ij}_{nm} = k^{ij}_{nm} n^{m-1}\left(\frac{a}{r_s}\right)^n \tag{152}$$

where $m = 2$ corresponds to the strike–slip, $m = 1$ to the dip–slip, and $m = 0$ to the horizontal and vertical tensile fracturings. Table 4 shows that even a linear interpolation of the transformed Love numbers gives accurate results.

4.5 Asymptotic solutions

We saw in Section 4.1 that the truncation degree N becomes too large for the infinite series to be accurately evaluated when $d_s < 1$ km. We introduce here the asymptotic solution technique to overcome the difficulty.

Okubo (1988) presented six independent sets of the asymptoic solutions for the spheroidal deformations of the earth. Recently he (Okubo 1993) also derived the

expressions of dislocation solutions, expressed simply by that of the tide, load and shear solutions. For convenience in our present study, we transform the asymptotic solutions into asymptotic dislocation Love numbers, $\tilde{h}^{ij}_{nm}$, $\tilde{l}^{ij}_{nm}$ and $\tilde{k}^{ij}_{nm}$ defined by (39)–(41). Using the Okubo's asymptotic solutions (or asymptotic dislocation Love numbers), we may speed up the convergence of the series.

For example, let us consider the radial displacement caused by a vertical strike–slip dislocation (from 64)

$$a^2\hat{u}_r^{12}(a,\theta) = 2\sum_{n=2}^{\infty} h_{n2}^{12}P_n^2(\cos\theta) = 2\sum_{n=2}^{\infty}\tilde{h}_{n2}^{12}P_n^2(\cos\theta) + 2\sum_{n=2}^{\infty}(h_{n2}^{12}-\tilde{h}_{n2}^{12})P_n^2(\cos\theta). \tag{153}$$

Since

$$\tilde{h}_{n2}^{12} = \left(\frac{r_s}{a}\right)^{n-1} y_{230}^{12} + \frac{1}{n}\left(\frac{r_s}{a}\right)^{n-1} y_{231}^{12} + \frac{1}{n^2}\left(\frac{r_s}{a}\right)^{n-1} y_{232}^{12} \tag{154}$$

(Appendix B), we have

$$\begin{aligned} a^2\hat{u}_r^{12}(a,\theta) = 2\sum_{n=2}^{\infty}&\left[y_{230}^{12}\left(\frac{r_s}{a}\right)^{n-1} + y_{231}^{12}\frac{1}{n}\left(\frac{r_s}{a}\right)^{n-1} + y_{232}^{12}\frac{1}{n(n+1)}\left(\frac{r_s}{a}\right)^{n-1}\right]P_n^2(\cos\theta) + 2 \\ &\times\sum_{n=2}^{\infty}\left[h_{n2}^{12} - y_{230}^{12}\left(\frac{r_s}{a}\right)^{n-1} - y_{231}^{12}\frac{1}{n}\left(\frac{r_s}{a}\right)^{n-1} - y_{232}^{12}\frac{1}{n(n+1)}\left(\frac{r_s}{a}\right)^{n-1}\right]P_n^2(\cos\theta). \end{aligned} \tag{155}$$

The first series on the right-hand side is evaluated analytically by substituting $t = (r_s/a)$ into the formulae in Appendix C. It follows

$$\begin{aligned} a^2\hat{u}_r^{12}(a,\theta) = {}& 2y_{230}^{12}\left(\frac{r_s}{a}\right)\frac{3\left(\frac{r_s}{a}\right)\sin^2\theta}{\left[1-2\left(\frac{r_s}{a}\right)+\left(\frac{r_s}{a}\right)^2\right]^{5/2}} \\ &+ 2y_{231}^{12}\frac{1}{\left(\frac{r_s}{a}\right)}\left[\frac{2}{\sin^2\theta} - 1 - \frac{1-\left(\frac{r_s}{a}\right)\cos\theta}{\left[1-2\cos^2\theta+\left(\frac{r_s}{a}\right)^2\right]^{3/2}}\right. \\ &\left. + \frac{2\cos\theta\left[\left(\frac{r_s}{a}\right)-\cos\theta\right]}{\sin^2\theta\sqrt{1-2\cos^2\theta+\left(\frac{r_s}{a}\right)^2}}\right] + 2y_{232}^{12}\frac{1}{\left(\frac{r_s}{a}\right)} \\ &\times\left\{1 - \frac{1}{\sqrt{1-2\left(\frac{r_s}{a}\right)\cos\theta+\left(\frac{r_s}{a}\right)^2}} - \frac{2\cos\theta}{\left(\frac{r_s}{a}\right)\sin^2\theta}\right. \\ &\left.\times\left[1-\left(\frac{r_s}{a}\right)\cos\theta - \sqrt{1-2\left(\frac{r_s}{a}\right)\cos\theta+\left(\frac{r_s}{a}\right)^2}\right]\right\} \\ &+ 2\sum_{n=2}^{\infty}\left[h_{n2}^{12} - y_{230}^{12}\left(\frac{r_s}{a}\right)^{n-1} - y_{231}^{12}\frac{1}{n}\left(\frac{r_s}{a}\right)^{n-1}\right. \\ &\left. - y_{232}^{12}\frac{1}{n(n+1)}\left(\frac{r_s}{a}\right)^{n-1}\right]P_n^2(\cos\theta). \end{aligned} \tag{156}$$

Notice that the infinite series on the right-hand side now converges quickly because the summand is $0(1/n)\cdot(r_s/a)^n$.

Similarly, we may obtain the expressions of other dislocations by referring to Appendices B and C.

5 COMPUTATIONAL RESULTS

We compute the gravity and potential changes due to dislocations in a homogeneous and a radially heterogeneous earth models.

5.1 Results for a homogeneous earth model

We present results for a homogeneous earth model defined by

$$\rho_0 = 2.183\times10^3\ \mathrm{kg\,m^{-3}}$$
$$\mu = 1.45\times10^{10}\ \mathrm{N\,m^{-2}}$$
$$\lambda = 1.90\times10^{10}\ \mathrm{N\,m^{-2}}$$
$$g_0 = 9.82\ \mathrm{m\,s^{-2}}$$
$$a = 6.371\times10^3\ \mathrm{km}.$$

These parameters are taken from the top layer of the 1066A earth model (Gilbert & Dziewonski 1975).

We have considered following source depths: 0, 2, 5, 10, 20, 32, 64, 100, 200, 300, 400 and 637 km. Numerical integrations were carried out to obtain the dislocation Love numbers by using the Runge–Kutta scheme.

Once we obtain the dislocation Love numbers, it is straightforward to calculate u_r, ψ, Δg and δg as described in Section 3. Figs 5(a) and 5(b) show the global gravity change on the free surface caused by a vertical strike–slip dislocation on the polar axis at depth of 32 km.

In these figures, the upper hemisphere is mapped onto a tangent plane at the epicentre. Each point on the hemisphere is moved to the tangent plane in such a way that the epicentre distance is preserved. The lower hemisphere is mapped similarly on the same plane. Note that the angle ϕ runs in a counter-clockwise direction on both upper and lower hemisphere maps. This means that in both cases we are looking at the sphere from a point above the upper hemisphere.

We see in Fig. 5(a) that the gravity change shows a quadrant pattern. Since the earth's surface in the quadrants 1 and 3 rises, the gravity should decrease, and vice versa.

It is of special interest to compare our results with solution for the half-space given by Okubo (1991). The distance x on the free surface of the half-space is related to its image on the sphere through the relation $x = a\theta$. The two results agree very well with each other within the epicentral distance $\theta < 1°$ or 111 km (Figs 5c and 6a). It verifies simultaneously that our theory is consistent with Okubo's flat-earth theory.

The discrepancy between the two results is no larger than 10 per cent within the epicentral distance $\theta = 10°$ (Figs 6b and 5a). The difference becomes evident when $\theta > 10°$ because of the curvature of the earth. It is reasonable to use the spherical theory for global calculation.

In Fig. 7, we present the gravity change caused by a dip–slip dislocation buried at $d_s = 32$ km. It shows a different pattern from that of the strike–slip. The outer circle in Fig. 7 is the line of epicentral distance 10°. The

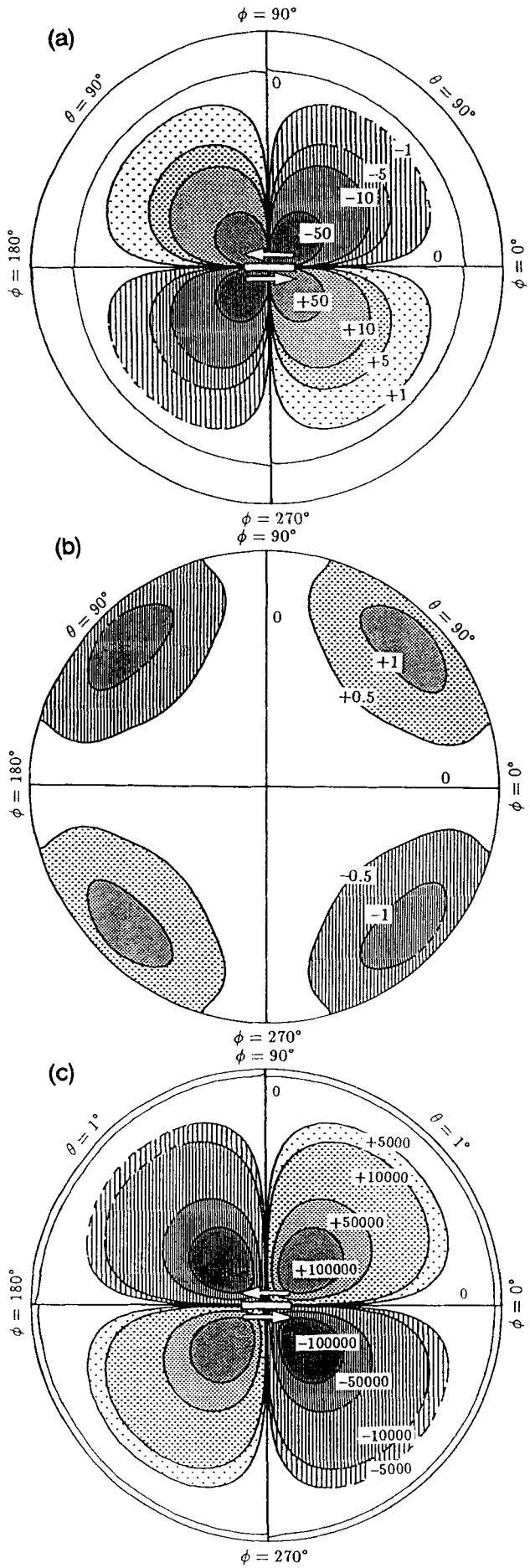

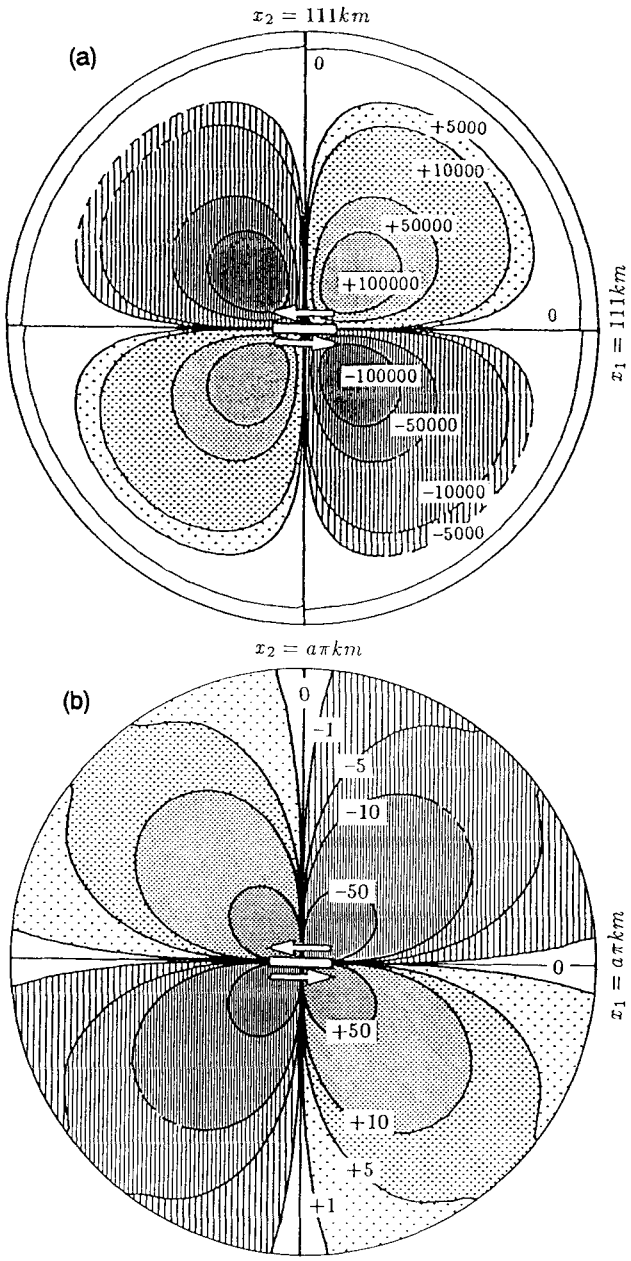

Figure 6. Gravity changes obtained from Okubo's (1991) theory due to a strike–slip dislocation in a flat-earth model. The depth of the dislocation is 32 km. The dislocation is $UdS = 2.49 \times 10^{13}$ m^3. The units are 'μ gal'. (a) $x < 111$ km. (b) $x < a\pi$ km.

Figure 5. Gravity changes due to a strike–slip dislocation in a homogeneous earth model. The epicentral distance is proportional to the radial distance. The depth of the dislocation is 32 km. The seismic moment is $M_{12} = 3.61 \times 10^{23}$ N · m, or $UdS = 2.49 \times 10^{13}$ m^3. The units are 'μgal'. (a) The upper hemisphere ($0° < \theta < 90°$). We find the positive gravity change in $90° < \phi < 180°$ and $270° < \phi < 360°$. A negative gravity change arises in $0° < \phi < 90°$ and $180° < \phi < 270°$. (b) The lower hemisphere ($90° < \theta < 180°$) with positive gravity change in $0° < \phi < 90°$ and $180° < \phi < 270°$, and negative gravity change in $90° < \phi < 180°$ and $270° < \phi < 360°$. (c) The near field ($0° < \theta < 1°$). It shows positive gravity change in $0° < \phi < 90°$ and $180° < \phi < 270°$. A negative gravity change arises in $90° < \phi < 180°$ and $270° < \phi < 360°$.

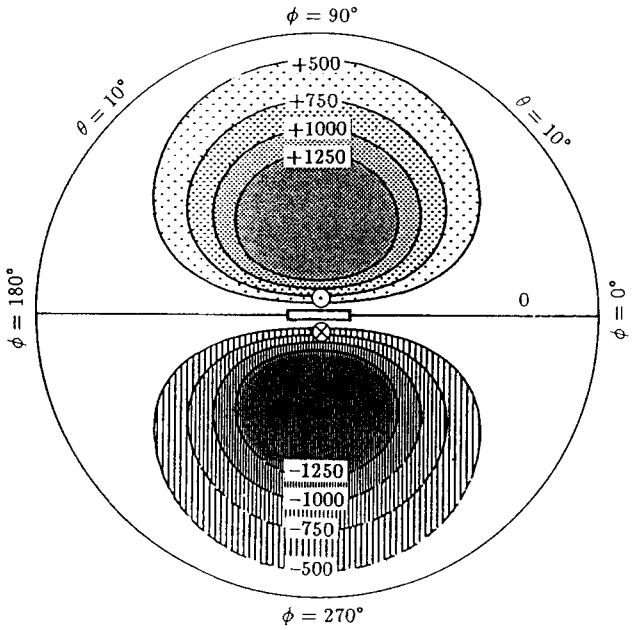

Figure 7. Gravity changes caused by a dip–slip dislocation in a homogeneous earth model. The epicentral distance is proportional to the radial distance. The solid line (with point shadow) denotes the positive gravity change, and the broken line (with line shadow) denotes the negative gravity change. The seismic moment is $M_{13} = 3.61 \times 10^{23}$ N · m, or $UdS = 2.49 \times 10^{13}$ m^3. The units are 'μ gal'. $0° < \theta < 10°$. The depth of the dislocation is 637 km.

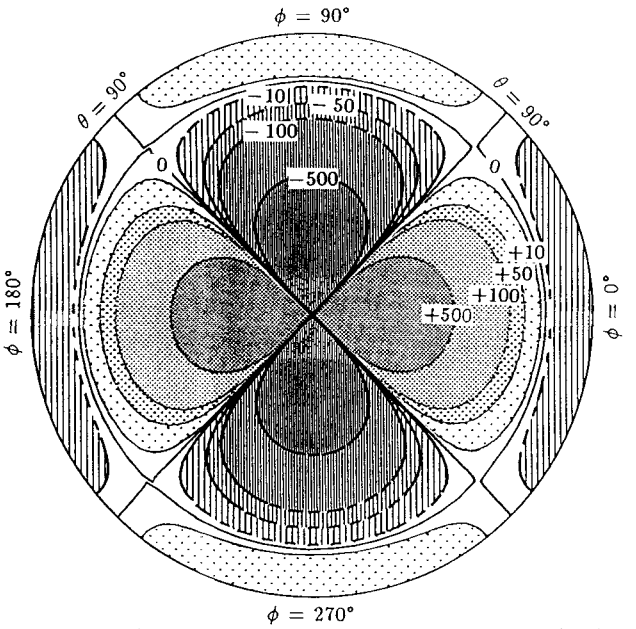

Figure 8. Gravity changes caused by a 45° dip–slip dislocation in a homogeneous earth model. The epicentral distance is proportional to the radial distance. The solid line (with point shadow) denotes the positive gravity change, and the broken line (with line shadow) denotes the negative gravity change. The seismic moment is $M_{13} = 3.61 \times 10^{24}$ N · m, or $UdS = 2.49 \times 10^{13}$ m^3. The units are 'μ gal'. $0° < \theta < 90°$. The depth of the dislocation is 32 km.

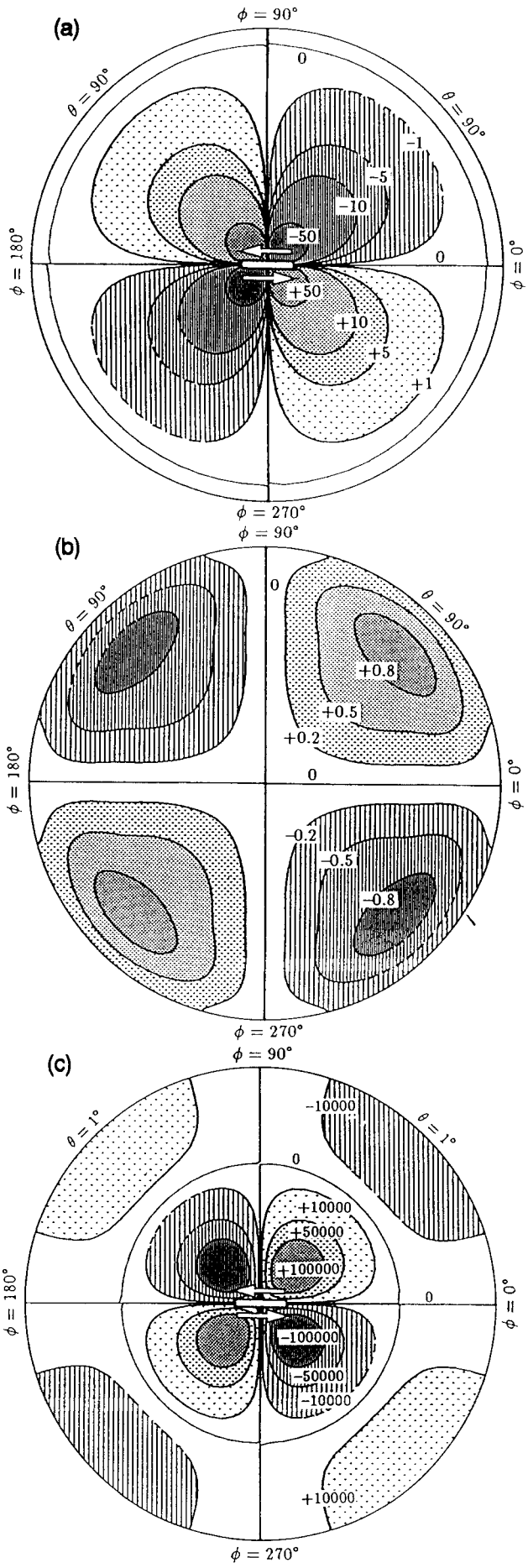

Figure 9. Gravity changes caused by a strike–slip dislocation in the 1066A earth model. The depth of the dislocation is 32 km. The solid line (with dotted shadow) denotes the positive gravity change, and the broken line (with line shadow) the negative gravity change. The dislocation in $u_1 n_2 dS = 2.49 \times 10^{13}$ m^3. The units are 'μ gal'. (a) The upper hemisphere ($0° < \theta < 90°$). (b) The lower hemisphere ($90° < \theta < 180°$). (c) The near field ($0° < \theta < 1°$).

gravity increases in the upper half part of the figure and decreases in the lower half.

We show the gravity change raised by a 45° dip-slip dislocation buried at $d_s = 32$ km in Fig. 8, where the outer circle is the line of epicentral distance 90°. It shows a quadrant pattern similar to that of the strike-slip dislocation, apart from a 45° phase difference in longitude.

5.2 Results for a radially heterogeneous earth model

Let us now turn to a more realistic problem: spheroidal deformation excited by a point dislocation in a radially heterogeneous earth. Using the formulation and techniques in Sections 3 and 4, we calculate u_r, ψ, Δg and δg caused by dislocations buried in the 1066A SNREI model (Gilbert & Dziewonski 1975).

Table 5. Dislocation Love numbers of a vertical strike-slip faulting at depth of 2 km. Earth model is the 1066A.

n	$\bar{h}^{12}_{n2}$	$\bar{l}^{12}_{n2}$	$\bar{k}^{12}_{n2}$
2	.3071$E-3$	.3228$E-2$	.8550$E-3$
3	−.2822$E-3$	.2555$E-2$	.2283$E-3$
4	−.2489$E-3$	.2157$E-2$	.2107$E-3$
5	−.1942$E-3$	.1857$E-2$	.2182$E-3$
6	−.1642$E-3$	.1636$E-2$	.2102$E-3$
8	−.1408$E-3$	.1335$E-2$	.1785$E-3$
10	−.1323$E-3$	.1135$E-2$	.1486$E-3$
15	−.1242$E-3$	.8380$E-3$	.9494$E-4$
20	−.1204$E-3$	.6766$E-3$	.6087$E-4$
30	−.1106$E-3$	.5071$E-3$	.2541$E-4$
40	−.9828$E-4$	.4176$E-3$	.1106$E-4$
50	−.8642$E-4$	.3612$E-3$	.5206$E-5$
70	−.6741$E-4$	.2931$E-3$	.2278$E-5$
100	−.4879$E-4$	.2378$E-3$	.3329$E-5$
200	−.2196$E-4$	.1613$E-3$	.8800$E-5$
300	−.1142$E-4$	.1254$E-3$	.1180$E-4$
500	−.2867$E-5$	.8372$E-4$	.1334$E-4$
800	.6922$E-6$	.5197$E-4$	.1177$E-4$
1000	.1478$E-5$	.4028$E-4$	.1046$E-4$
1200	.2033$E-5$	.3231$E-4$	.9429$E-5$
1400	.2586$E-5$	.2652$E-4$	.8693$E-5$
1600	.3180$E-5$	.2207$E-4$	.8205$E-5$
1800	.3794$E-5$	.1852$E-4$	.7893$E-5$
2000	.4397$E-5$	.1561$E-4$	.7700$E-5$
2200	.4968$E-5$	.1317$E-4$	.7583$E-5$
2400	.5494$E-5$	.1111$E-4$	.7512$E-5$
2600	.5971$E-5$	.9345$E-5$	.7470$E-5$
2800	.6400$E-5$	.7814$E-5$	.7445$E-5$
3000	.6784$E-5$	.6478$E-5$	.7430$E-5$
3500	.7577$E-5$	.3786$E-5$	.7414$E-5$
4000	.8186$E-5$	.1756$E-5$	.7410$E-5$
4500	.8663$E-5$	.1737$E-6$	.7410$E-5$
5000	.9046$E-5$	−.1093$E-5$	.7410$E-5$
7000	.1003$E-4$	−.4351$E-5$	.7411$E-5$
10000	.1077$E-4$	−.6795$E-5$	.7412$E-5$
15000	.1134$E-4$	−.8696$E-5$	.7413$E-5$
20000	.1163$E-4$	−.9647$E-5$	.7414$E-5$
25000	.1180$E-4$	−.1021$E-4$	.7414$E-5$
30000	.1192$E-4$	−.1059$E-4$	.7414$E-5$
35000	.1201$E-4$	−.1088$E-4$	.7420$E-5$

We first calculate dislocation Love numbers (see, as examples, Tables 5–8). Final results on displacement u_r, potential ψ and gravity changes Δg and δg are tabulated in Appendix A.

Fig. 9 shows the gravity changes raised by a strike-slip dislocation at a depth of 32 km. We observe a slight difference between this result and that for the homogeneous earth model (Fig. 5a), although the distribution patterns and numerical order remain essentially the same.

Fig. 9(c) shows the gravity changes in the near field raised by the same dislocation. The result for the 1066A model is as a whole similar to that for a homogeneous sphere (Figs 9c and 5c). At some places, however, the difference between the two becomes very large. For example, the locations of the nodal lines of the gravity change differ significantly between the two models. For more detailed comparison, we show results of the homogeneous and 1066A models in Fig. 10. Fig. 10 clearly indicates that the vertical layering can cause considerable effects on the deformation fields. The distribution pattern and numerical order are, however, basically the same within $0° < \theta < 0.5°$. Since the top 11 km of the earth model 1066A is homogeneous adopted as our homogeneous model (previous section), there should be no large difference between the two models when epicentral

Table 6. Dislocation Love numbers of a vertical dip-slip faulting at depth of 20 km. Earth model is the 1066A.

n	$\bar{h}^{32}_{n1}$	$\bar{l}^{32}_{n1}$	$\bar{k}^{32}_{n1}$
1	−.5345$E-4$	.6014$E-1$	.0000$E+0$
2	.1097$E-3$	.3350$E-1$	.1621$E-3$
3	.1224$E-3$	.2344$E-1$	.1695$E-3$
4	.1186$E-3$	.1807$E-1$	.1617$E-3$
5	.1146$E-3$	.1472$E-1$	.1547$E-3$
6	.1131$E-3$	.1242$E-1$	.1505$E-3$
8	.1146$E-3$	.9470$E-2$	.1469$E-3$
10	.1182$E-3$	.7649$E-2$	.1460$E-3$
15	.1295$E-3$	.5161$E-2$	.1486$E-3$
20	.1417$E-3$	.3887$E-2$	.1542$E-3$
30	.1626$E-3$	.2588$E-2$	.1661$E-3$
40	.1772$E-3$	.1926$E-2$	.1750$E-3$
50	.1871$E-3$	.1523$E-2$	.1809$E-3$
70	.1992$E-3$	.1055$E-2$	.1873$E-3$
100	.2087$E-3$	.6942$E-3$	.1910$E-3$
200	.2257$E-3$	.2395$E-3$	.1924$E-3$
300	.2387$E-3$	.6409$E-4$	.1911$E-3$
400	.2510$E-3$	−.3349$E-4$	.1903$E-3$
500	.2636$E-3$	−.9637$E-4$	.1909$E-3$
800	.3036$E-3$	−.2017$E-3$	.2006$E-3$
1000	.3295$E-3$	−.2440$E-3$	.2106$E-3$
1200	.3522$E-3$	−.2762$E-3$	.2206$E-3$
1400	.3705$E-3$	−.3014$E-3$	.2292$E-3$
1600	.3843$E-3$	−.3210$E-3$	.2358$E-3$
1800	.3943$E-3$	−.3361$E-3$	.2407$E-3$
2000	.4013$E-3$	−.3477$E-3$	.2441$E-3$
2200	.4063$E-3$	−.3568$E-3$	.2464$E-3$
2400	.4098$E-3$	−.3640$E-3$	.2481$E-3$
2600	.4124$E-3$	−.3698$E-3$	.2492$E-3$
2800	.4143$E-3$	−.3746$E-3$	.2500$E-3$
3000	.4159$E-3$	−.3787$E-3$	.2507$E-3$
3500	.4198$E-3$	−.3877$E-3$	.2525$E-3$

Table 7. Dislocation Love numbers of a horizontal tensile at depth of 200 km. Earth model is the 1066A.

n	$\bar{h}^{22}_{n0}$	$\bar{l}^{22}_{n0}$	$\bar{k}^{22}_{n0}$
0	.5592E − 01	.0000E + 0	.0000E + 0
1	.1675E + 00	−.1550E + 0	.0000E + 0
2	.1041E + 00	−.7161E − 1	.3139E − 1
3	.5916E − 01	−.5626E − 1	.1225E − 1
4	.3811E − 01	−.4349E − 1	.3653E − 2
5	.2757E − 01	−.3502E − 1	.3573E − 3
6	.2163E − 01	−.2941E − 1	−.9092E − 3
8	.1524E − 01	−.2245E − 1	−.1648E − 2
10	.1178E − 01	−.1817E − 1	−.1802E − 2
15	.7360E − 02	−.1210E − 1	−.1819E − 2
20	.5152E − 02	−.8865E − 2	−.1784E − 2
25	.3774E − 02	−.6823E − 2	−.1782E − 2
30	.2805E − 02	−.5401E − 2	−.1809E − 2
35	.2075E − 02	−.4344E − 2	−.1850E − 2
40	.1503E − 02	−.3521E − 2	−.1897E − 2
45	.1043E − 02	−.2860E − 2	−.1942E − 2
50	.6647E − 03	−.2315E − 2	−.1984E − 2
60	.8140E − 04	−.1468E − 2	−.2053E − 2
70	−.3449E − 03	−.8365E − 3	−.2105E − 2
80	−.6689E − 03	−.3437E − 3	−.2142E − 2
90	−.9231E − 03	.5360E − 4	−.2169E − 2
100	−.1128E − 02	.3827E − 3	−.2188E − 2
110	−.1296E − 02	.6613E − 3	−.2202E − 2
120	−.1438E − 02	.9014E − 3	−.2211E − 2
130	−.1560E − 02	.1111E − 2	−.2217E − 2
140	−.1665E − 02	.1297E − 2	−.2221E − 2
150	−.1758E − 02	.1464E − 2	−.2224E − 2
160	−.1841E − 02	.1614E − 2	−.2225E − 2
170	−.1915E − 02	.1751E − 2	−.2225E − 2
180	−.1982E − 02	.1876E − 2	−.2225E − 2
200	−.2100E − 02	.2097E − 2	−.2222E − 2
300	−.2513E − 02	.2851E − 2	−.2206E − 2

Table 8. Dislocation Love numbers of an opening tensile crack at depth of 400 km. Earth model is the 1066A.

n	$\bar{h}^{33}_{n0}$	$\bar{l}^{33}_{n0}$	$\bar{k}^{33}_{n0}$
0	.8791E − 1	.0000E + 0	.0000E + 0
1	.2689E + 0	−.2612E − 1	.0000E + 0
2	.1235E + 0	−.1438E − 1	.1045E − 1
3	.8104E − 1	−.1373E − 1	.9993E − 2
4	.6190E − 1	−.1344E − 1	.9975E − 2
5	.5115E − 1	−.1335E − 1	.1006E − 1
6	.4430E − 1	−.1333E − 1	.1015E − 1
8	.3611E − 1	−.1336E − 1	.1032E − 1
10	.3145E − 1	−.1343E − 1	.1049E − 1
15	.2569E − 1	−.1374E − 1	.1093E − 1
20	.2307E − 1	−.1410E − 1	.1129E − 1
25	.2158E − 1	−.1443E − 1	.1153E − 1
30	.2059E − 1	−.1472E − 1	.1168E − 1
35	.1987E − 1	−.1495E − 1	.1176E − 1
40	.1931E − 1	−.1516E − 1	.1179E − 1
45	.1886E − 1	−.1535E − 1	.1180E − 1
50	.1850E − 1	−.1552E − 1	.1179E − 1
60	.1793E − 1	−.1584E − 1	.1174E − 1
70	.1752E − 1	−.1614E − 1	.1167E − 1
80	.1721E − 1	−.1641E − 1	.1160E − 1
90	.1697E − 1	−.1668E − 1	.1152E − 1
100	.1679E − 1	−.1694E − 1	.1146E − 1
110	.1665E − 1	−.1719E − 1	.1139E − 1
120	.1655E − 1	−.1745E − 1	.1133E − 1
130	.1648E − 1	−.1772E − 1	.1128E − 1
140	.1645E − 1	−.1806E − 1	.1124E − 1
150	.1643E − 1	−.1852E − 1	.1119E − 1
160	.1598E − 1	−.1791E − 1	.1087E − 1

distance is less than 1 km. The effect of the vertical layering becomes more evident when $\theta > 0.1°$.

We give some results for inclined dislocations in Figs 11–14. They show more complicated patterns, which strongly depend on the dip angle δ and slip angle λ. (See Sun (1992) for more complete results for u_r, ψ and Δg).

6 CONCLUSIONS

We showed how to compute the potential and gravity changes caused by point dislocations in spherically symmetric earth.

Although our formulation is rather simple, we had to overcome several difficulties to obtain numerical results: (1) truncation of an infinite series, (2) accelerating the convergence of the series, (3) the Euler transformation, (4) interpolation on transformed Love numbers, and (5) incorporation of Okubo's (1988, 1991c) asymptotic solutions.

We made calculations for both homogeneous and radially heterogeneous earth models. Numerical integrations were carried out by using Runge–Kutta method. For depths of 0, 2, 5, 10, 20, 32, 64, 100, 200, 300, 400, 637 km, we obtained the dislocation Love numbers, which enable us to calculate radial displacement, potential and gravity changes. Calculated gravity changes for a homogeneous sphere agree well with previous results derived from the assumption of a homogeneous flat earth, in particular in the near field within 1° or 111 km. The agreement confirms that our theory is consistent with the flat-earth theory (Okubo 1991). Discrepancy between the two theories was found to be no larger than 10 per cent within epicentral distance $\theta \approx 10°$. The difference becomes larger in the area $\theta > 10°$, where the effect of the curvature appears evident.

We proceeded to calculations for the radially heterogeneous 1066A earth model. The results are as a whole similar to those for a homogeneous sphere. In some cases, however, the difference between the two becomes very large. For example, the locations of the nodal lines of the gravity change differ significantly between the two models. It indicates that the vertical layering has considerable effects on the deformation fields.

The most important results of this study are the radial displacement, potential and gravity changes tabulated in Appendix A. These results enable us to compute potential and gravity changes at any place on the surface due to an arbitrary point dislocation in a SNREI earth.

If we integrate the contribution from point dislocations distributed over a finite plane, we may estimate gravity change caused by an earthquake more accurately. We will show how this is achieved in the subsequent paper (Okubo & Sun 1993).

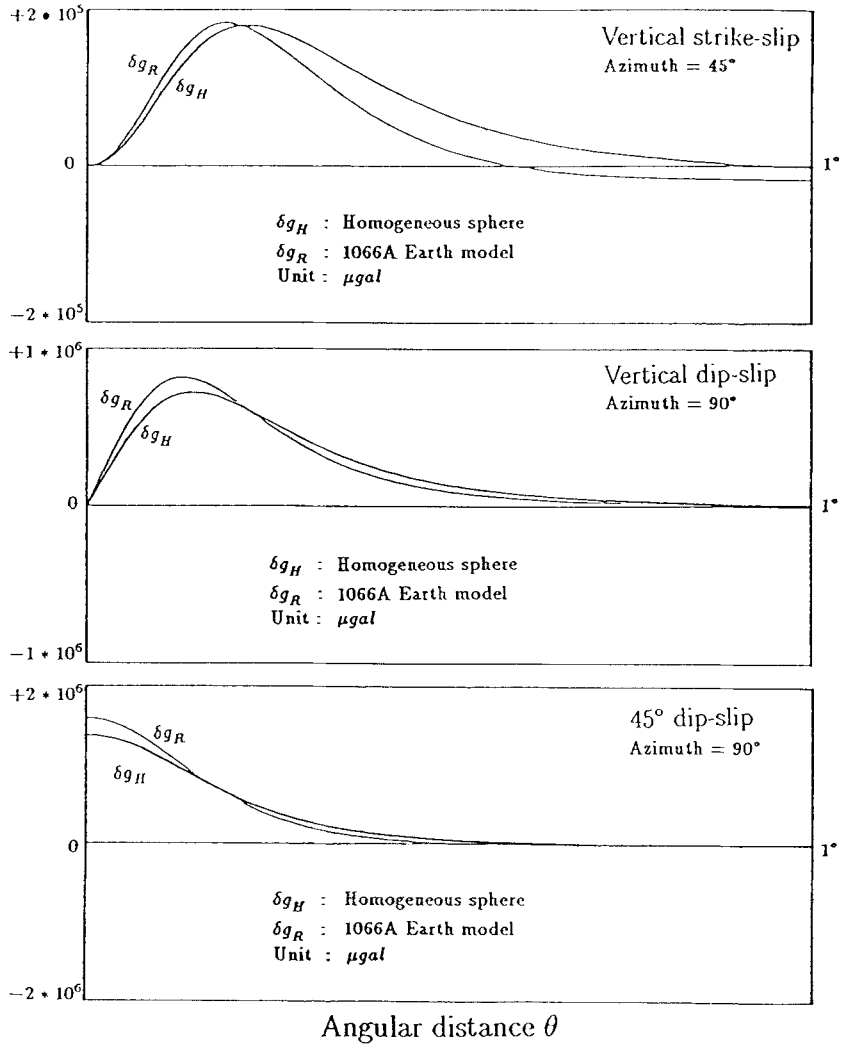

Figure 10. Comparison of gravity changes of the homogeneous and 1066A models.

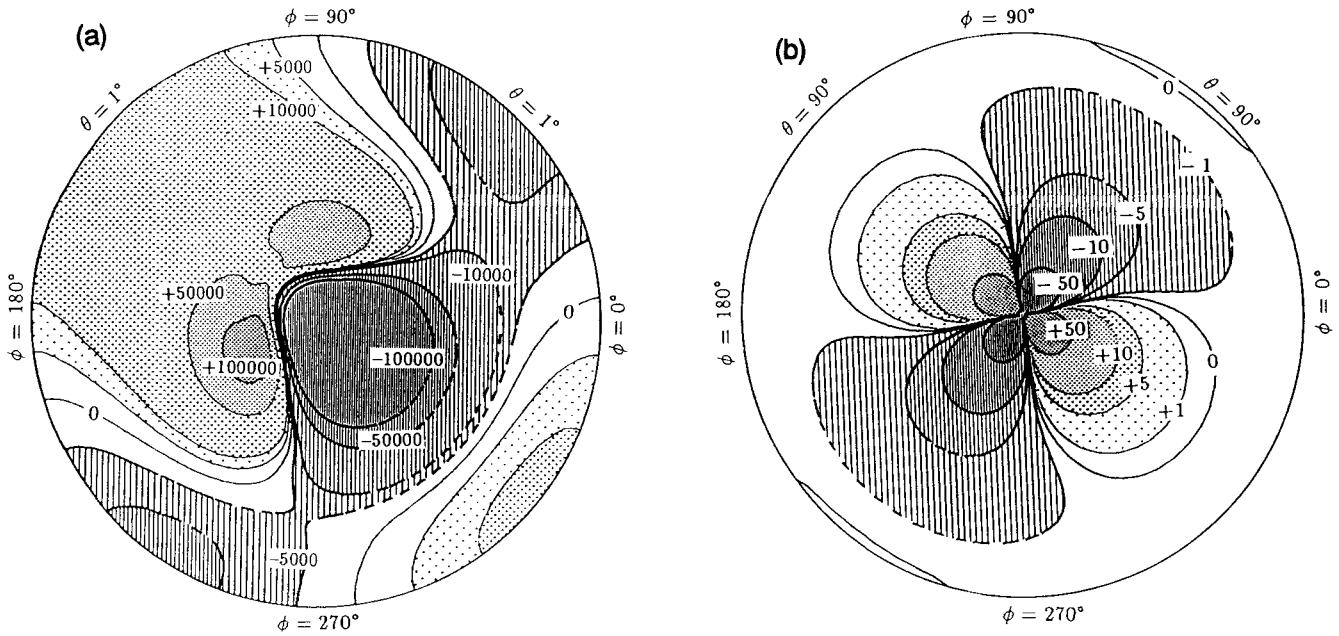

Figure 11. Gravity changes δg (with the free air correction) caused by a shear dislocation ($\delta = 60°$, $\lambda = 30°$, $d_s = 32$ km) in the 1066A earth model. The dislocation is located at the centre of the map. The epicentral distance is proportional to the radial distance. The dislocation is $UdS = 2.49 \times 10^{13}$ m^3. The units are 'μ gal'. (a) The near field ($0° < \theta < 1°$). (b) The upper hemisphere ($0° < \theta < 90°$). (c) The lower hemisphere ($90° < \theta < 180°$).

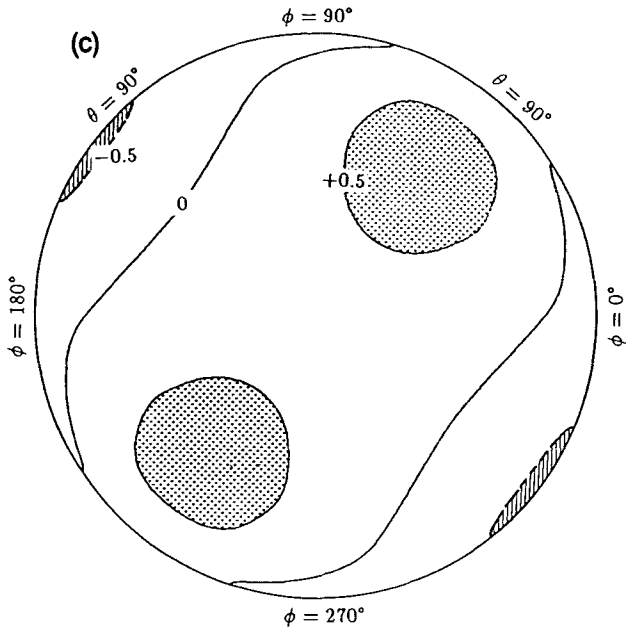

Figure 11. (*Continued.*)

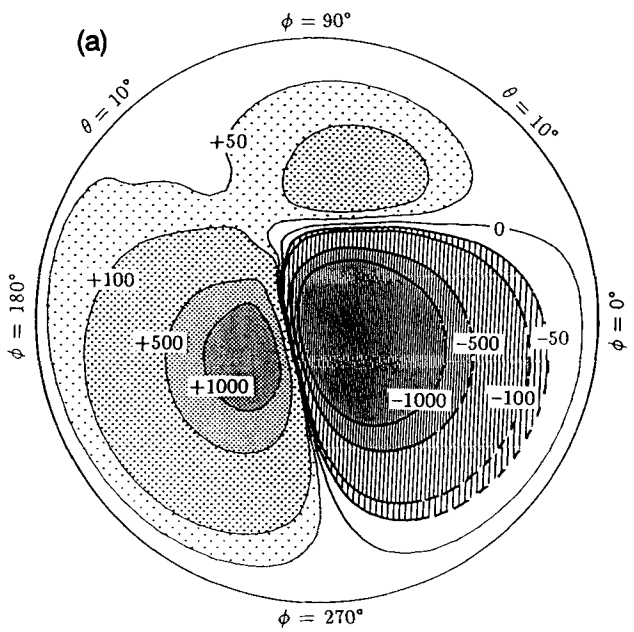

Figure 12.

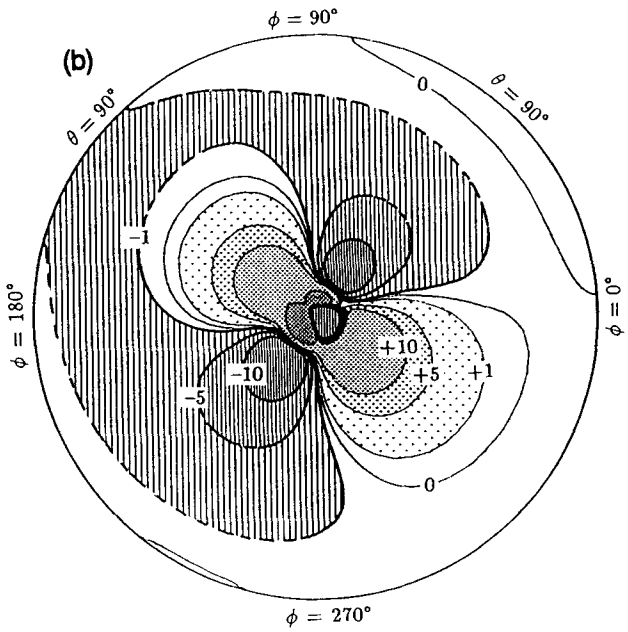

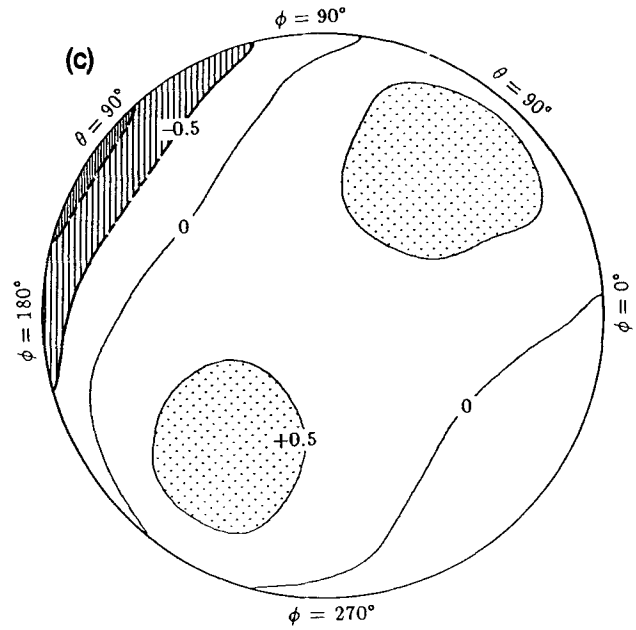

Figure 12. Gravity changes δg (with the free air correction) caused by a shear dislocation ($\delta = 50°$, $\lambda = 20°$, $d_s = 400$ km) in the 1066A earth model. The dislocation is located at the centre of the map. The epicentral distance is proportional to the radial distance. The dislocation is $UdS = 2.49 \times 10^{13}$ m^3. The units are 'μ gal'. (a) The near field ($0° < \theta < 10°$). (b) The upper hemisphere ($0° < \theta < 90°$). (c) The lower hemisphere ($90° < \theta < 180°$).

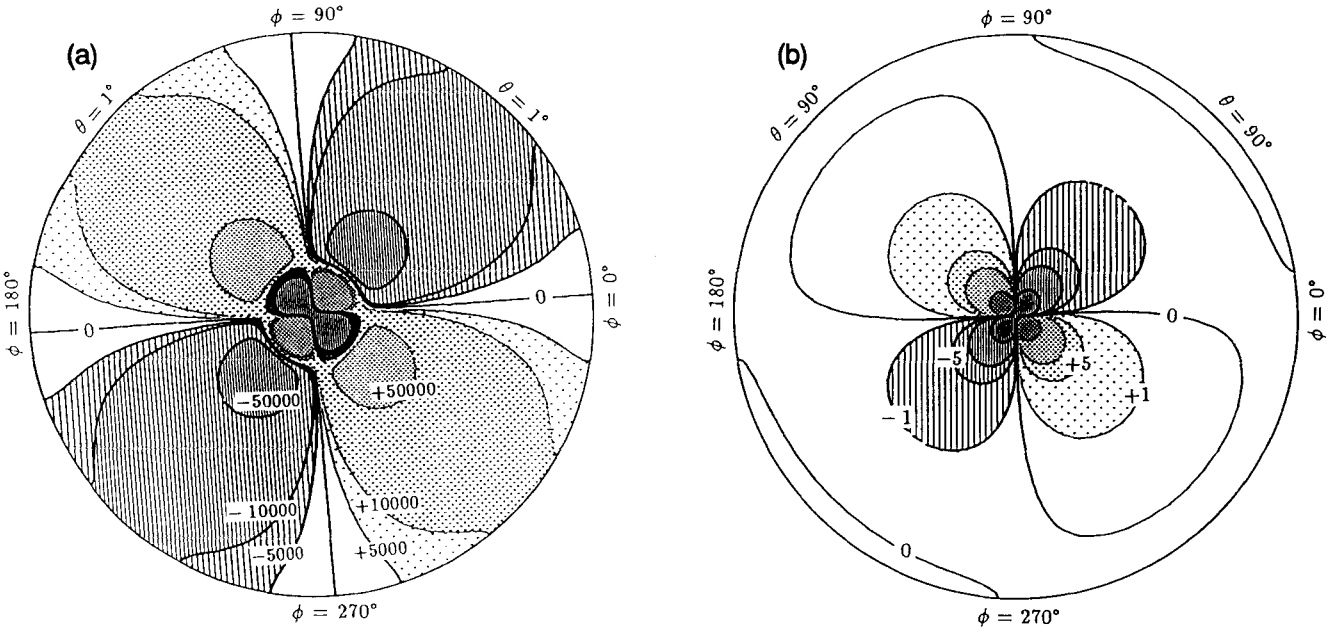

Figure 13. Gravity changes δg (with the free air correction) caused by a shear dislocation ($\delta = 75°$, $\lambda = 15°$, $d_s = 5$ km) in the 1066A earth model. The dislocation is located at the centre of the map. The epicentral distance is proportional to the radial distance. The dislocation is $UdS = 2.49 \times 10^{13}$ m^3. The units are 'μ gal'. (a) The near field ($0° < \theta < 1°$). (b) The upper hemisphere ($0° < \theta < 90°$).

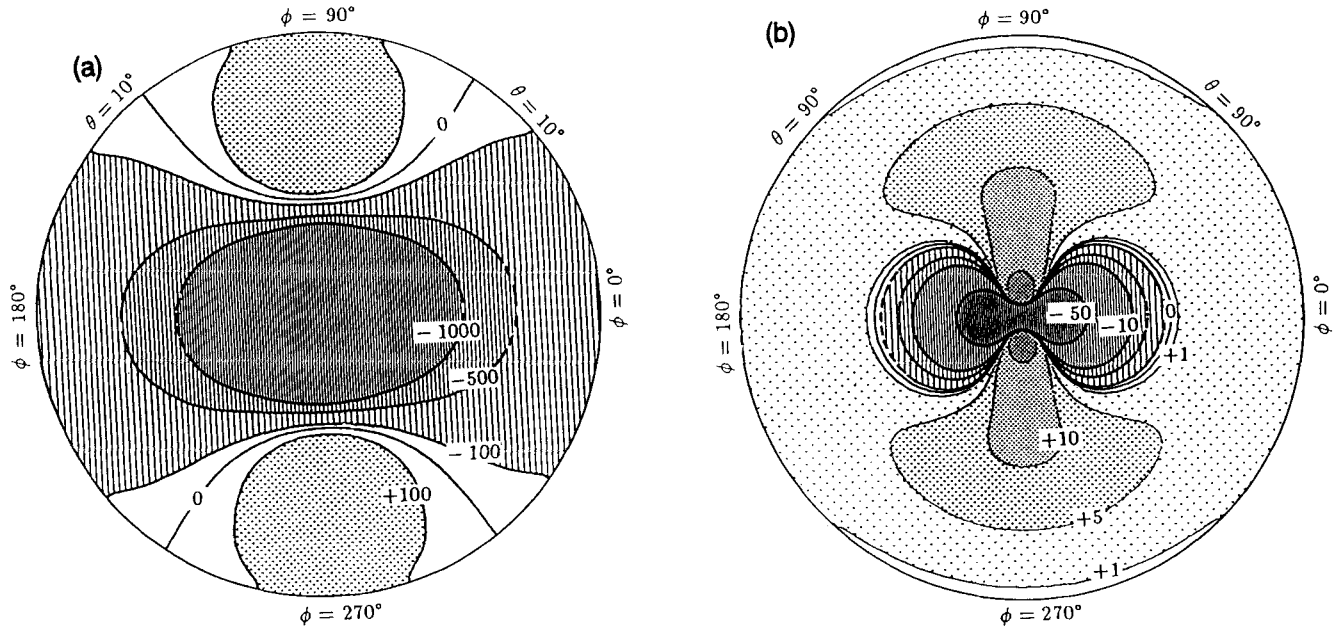

Figure 14. Gravity changes δg (with the free air correction) caused by a Tensile dislocation ($\delta = 90°$, $d_s = 100$ km) in the 1066A earth model. The dislocation is located at the centre of the map. The epicentral distance is proportional to the radial distance. The dislocation is $UdS = 2.49 \times 10^{13}$ m^3. The units are 'μ gal'. (a) The near field ($0° < \theta < 10°$). (b) The upper hemisphere ($0° < \theta < 90°$). (c) The lower hemisphere ($90° < \theta < 180°$).

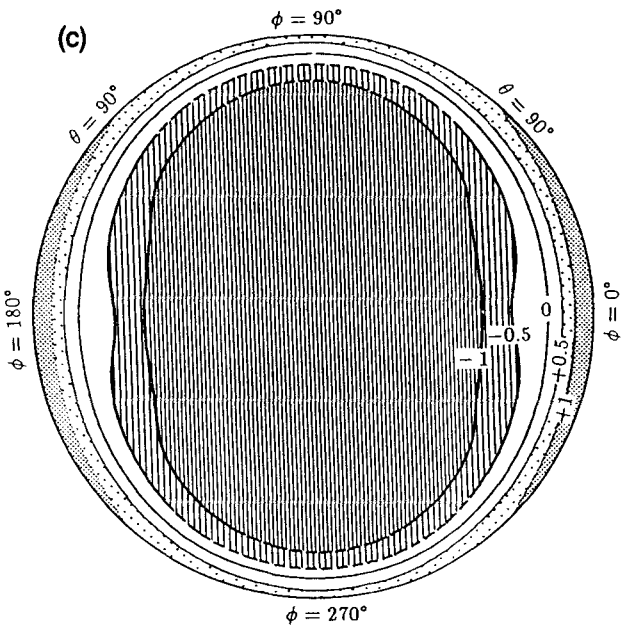

Figure 14. (*Continued.*)

ACKNOWLEDGMENTS

We would like to gratefully acknowledge the critical review by Professor K. Abe. We used HITAC M-680H computer system at the Earthquake Research Institute of the University of Tokyo. This research was carried out during WS's stay in Japan with a Japanese Government scholarship.

REFERENCES

Alterman, Z., Jarosch, H. & Pekeris, C. L., 1959. Oscillation of the earth, *Proc. R. Soc., Lond., Ser.* A, **252,** 80–95.

Ben-Menahem, A. & Singh, S. J., 1968. Eigenvector expansions of Green's dyads with applications to geophysical theory, *Geophy. J. R. astr. Soc.*, **16,** 417–452.

Ben-Menahem, A., Singh, S. J. & Solomon, F., 1969. Static deformation of a spherical earth model by internal dislocations, *Bull. seism. Soc. Am.*, **59,** 813–853.

Ben-Menahem, A. & Israel, M., 1970. Effects of major seismic events on the rotation of the earth, *Geophys. J. R. astr. Soc.*, **19,** 367–393.

Dahlen, F. A., 1968. The normal modes of a rotating, elliptical earth, *Geophys. J. R. astr. Soc.*, **16,** 329–367.

Farrell, W. E., 1972. Deformation of the earth by surface loads, *Rev. Geophys. Space Phys.*, **10,** 761–797.

Gilbert, F. & Dziewonski, A. M., 1975. An application of normal mode theory to the retrieval of structural parameters and source mechanisms from seismic spectra, *Phil. Trans. R. Soc. Lond., Ser.* A, **278,** 187–269.

Hagiwara, Y., 1977. The Mogi model as a possible cause of the crustal uplift in the eastern part of Izu Peninsula and the related gravity change, *Bull. Earthq. Res. Inst., Univ. Tokyo,* **52,** 301–309 (in Japanese with an English abstract).

Kagan, Y. Y., 1987a. Point sources of elastic deformation, elementary sources, static displacements, *Geophys. J. R. astr. Soc.*, **90,** 1–34.

Kagan, Y. Y., 1987b. Point sources of elastic deformation, elementary sources, dynamic displacements, *Geophys. J. R. astr. Soc.*, **91,** 891–912.

Longman, I. M., 1962. A Green's function for determining the deformation of the earth under surface mass loads, 1. Theory, *J. geophys. Res.*, **67,** 845–850.

Longman, I. M., 1963. A Green's function for determining the deformation of the earth under surface mass loads, 2. Computations and numerical results, *J. geophys. Res.*, **68,** 485–496.

Maruyama, T., 1964. Statical elastic dislocations in an infinite and semi-infinite medium, *Bull. Earthq. Res. Inst., Univ. Tokyo*, **42,** 289–368.

Okada, Y., 1985. Surface deformation due to shear and tensile faults in a half-space, *Bull. seism. Soc. Am.*, **75,** 1135–1154.

Okubo, S. & Endo, T., 1986. Static spheroidal deformation of degree 1—consistency relation, stress solution and partials, *Geophys. J. R. astr. Soc.*, **86,** 91–102.

Okubo, S., 1988. Asymptotic solutions to the static deformation of the earth—1. Spheroidal mode, *Geophys. J. Int.*, **92,** 39–51.

Okubo, S., 1991. Potential and gravity changes raised by point dislocations, *Geophys. J. Int.*, **105,** 573–586.

Okubo, S., 1992. Potential and gravity changes due to shear and tensile faults, *J. geophys. Res.*, **97,** 7137–7144.

Okubo, S., 1993. Reciprocity theorem to compute the static deformation due to a point dislocation buried in a spherically symmetric earth, *Geophys. J. Int.*, in press.

Okubo, S. & Sun, W., 1993. Surface potential and gravity changes due to internal dislocations in a spherical earth—2. Application, *Geophys. J. Int.*, submitted.

Press, F., 1965. Displacements, strains and tilts at teleseismic distances, *J. geophys. Res.*, **70,** 2395–2412.

Saito, M., 1967. Excitation of free oscillations and surface waves by a point source in a vertically heterogeneous earth, *J. geophys. Res.*, **72,** 3689–3699.

Saito, M., 1974. Some problems of static deformation of the earth, *J. Phys. Earth*, **22,** 123–140.

Satio, M., 1978. Relationship between tidal and load Love numbers, *J. Phys. Earth*, **26,** 13–16.

Sasai, Y., 1986. Multiple tension crack model for dilatacy, surface displacement, gravity and magnetic change, *Bull. Earthq. Res. Inst., Univ. Tokyo,* **61,** 429–473.

Sasai, Y., 1988. Correction to the paper 'Multiple tension crack model for dilatancy, surface displacement, gravity and magnetic change', *Bull. Earthq. Res. Inst., Univ. Tokyo,* **63,** 323–326.

Savage, J. C., 1984. Local gravity anomalies produced by dislocation sources, *J. geophys. Res.,* **89,** 1945–1952.

Smylie, D. S. & Mansinha, L., 1971. The elasticity theory of dislocation in real earth models and changes in the rotation of the earth, *Geophys. J. R. astr. Soc.,* **23,** 329–354.

Steketee, J. A., 1958. On Volterra's dislocations in a semi-infinite elastic medium, *Can. J. Phys.,* **36,** 192–205.

Sun, W., 1992. Potential and gravity changes raised by dislocations in spherically symmetric earth models, *PhD thesis,* The University of Tokyo, Japan.

Takeuchi, H. & Saito, M., 1972. Seismic surface waves, *Meth. comput. Phys.,* **11,** 217–295.

APPENDICES

A Tables of deformations caused by dislocations

In this Appendix we give the numerical results of the radial displacement $\hat{u}_r^{ij}(a, \theta)$, the potential change $\hat{\psi}^{ij}(a, \theta)$, the gravity changes $\Delta\hat{g}^{ij}(a, \theta)$ and $\delta\hat{g}^{ij}(a, \theta)$ for practical applications. (On microfiche GJI 114/1.)

B Asymptotic solutions

Okubo (1988) proposed the asymptotic solutions for the whole six sets of independent solutions of the spheroidal deformations of the earth. Recently he (Okubo 1993) found that the deformation on the surface $r = a$ raised by dislocations is expressed simply by that of the tide, load and shear solutions at the source depth d_s. For convenience in our present study, we transform the asymptotic solutions into asymptotic dislocation Love numbers: h_{nm}^{ij}, l_{nm}^{ij}, and k_{nm}^{ij}. The superscripts 'Tide', 'Load', and 'Shear' indicate the tide, the load, and the shear asymptotic solutions at the point source.

Vertical strike-slip

$$h_{n2}^{12} = -\frac{3}{8\pi\rho_0\xi}\frac{\mu_s}{r_s}[y_3^{\text{Load}}(r_s; n) - y_3^{\text{Tide}}(r_s; n)] = \left(\frac{r_s}{a}\right)^{n-1}\left(y_{230}^{12} + \frac{1}{n}y_{231}^{12} + \frac{1}{n^2}y_{232}^{12}\right) \tag{B1}$$

$$l_{n2}^{12} = \frac{3}{8\pi\rho_0\xi}\frac{\mu_s}{r_s}y_3^{\text{Shear}}(r_s; n) = \frac{1}{n}\left(\frac{r_s}{a}\right)^{n-1}\left(y_{330}^{12} + \frac{1}{n}y_{331}^{12} + \frac{1}{n^2}y_{332}^{12}\right) \tag{B2}$$

$$k_{n2}^{12} = \frac{Ga\mu_s}{2r_s}y_3^{\text{Tide}}(r_s; n) = \frac{1}{n}\left(\frac{r_s}{a}\right)^{n-1}\left(y_{130}^{12} + \frac{1}{n}y_{131}^{12} + \frac{1}{n^2}y_{132}^{12}\right) \tag{B3}$$

Vertical dip-slip

$$h_{n1}^{23} = -\frac{3}{8\pi\rho_0\xi}[y_4^{\text{Load}}(r_s; n) - y_4^{\text{Tide}}(r_s; n)] = n\left(\frac{r_s}{a}\right)^{n-2}\left(y_{240}^{23} + \frac{1}{n}y_{241}^{23}\right) \tag{B4}$$

$$l_{n1}^{23} = \frac{3}{8\pi\rho_0\xi}y_4^{\text{Shear}}(r_s; n) = \left(\frac{r_s}{a}\right)^{n-2}\left(y_{340}^{23} + \frac{1}{n}y_{341}^{23} + \frac{1}{n^2}y_{342}^{23}\right) \tag{B5}$$

$$k_{n1}^{23} = \frac{Ga}{2}y_4^{\text{Tide}}(r_s; n) = \left(\frac{r_s}{a}\right)^{n-2}\left(y_{140}^{23} + \frac{1}{n}y_{141}^{23}\right). \tag{B6}$$

Horizontal tensile fracturing with $m = 0$:

$$\begin{aligned} h_{n0}^{22} = &-\frac{3}{4\pi\rho_0\xi}\left[\frac{\lambda_s}{\sigma_s}[y_2^{\text{Load}}(r_s; n) - y_2^{\text{Tide}}(r_s; n)]\right. \\ &+\frac{3K_s}{\sigma_s}\frac{\mu_s}{r_s}[2[y_1^{\text{Load}}(r_s; n) - y_1^{\text{Tide}}(r_s; n)] \\ &\left.-n(n+1)[y_3^{\text{Load}}(r_s; n) - y_3^{\text{Tide}}(r_s; n)]]\right] \\ = &\, n^2\left(\frac{r_s}{a}\right)^{n-1}(y_{220}^{22} + y_{230}^{22}) \\ &+n\left(\frac{r_s}{a}\right)^{n-1}(y_{210}^{22} + y_{221}^{22} + y_{230}^{22} + y_{231}^{22}) \\ &+\left(\frac{r_s}{a}\right)^{n-1}(y_{211}^{22} + y_{222}^{22} + y_{231}^{22} + y_{232}^{22}) \end{aligned} \tag{B7}$$

$$\begin{aligned} l_{n0}^{22} = &\frac{3}{4\pi\rho_0\xi}\left\{\frac{\lambda_s}{\sigma_s}y_2^{\text{Shear}}(r_s; n) + \frac{3K_s}{\sigma_s}\frac{\mu_s}{r_s}\right. \\ &\left.\times[2y_1^{\text{Shear}}(r_s; n) - n(n+1)y_3^{\text{Shear}}(r_s; n)]\right\} \\ = &\, n\left(\frac{r_s}{a}\right)^{n-1}(y_{320}^{22} + y_{330}^{22}) + \left(\frac{r_s}{a}\right)^{n-1} \\ &\times(y_{310}^{22} + y_{321}^{22} + y_{330}^{22} + y_{331}^{22}) + \frac{1}{n}\left(\frac{r_s}{a}\right)^{n-1} \\ &\times(y_{311}^{22} + y_{331}^{22} + y_{332}^{22}) \end{aligned} \tag{B8}$$

$$\begin{aligned} k_{n0}^{22} = &\, Ga\left\{\frac{\lambda_s}{\sigma_s}y_2^{\text{Tide}}(r_s; n) + \frac{3K_s}{\sigma_s}\frac{\mu_s}{r_s}\right. \\ &\left.\times[2y_1^{\text{Tide}}(r_s; n) - n(n+1)y_3^{\text{Tide}}(r_s; n)]\right\} \\ = &\, n\left(\frac{r_s}{a}\right)^{n-1}(y_{120}^{22} + y_{130}^{22}) + \left(\frac{r_s}{a}\right)^{n-1}(y_{110}^{22} + y_{130}^{22} + y_{131}^{22}) \\ &+\frac{1}{n}\left(\frac{r_s}{a}\right)^{n-1}(y_{111}^{22} + y_{131}^{22} + y_{132}^{22}). \end{aligned} \tag{B9}$$

Vertical tensile fracturing

$$h_{n0}^{33} = -\frac{3}{4\pi\rho_0\xi}[y_2^{\text{Load}}(r_s; n) - y_2^{\text{Tide}}(r_s; n)] = \left(\frac{r_s}{a}\right)^{n-2}(n^2y_{220}^{33} + ny_{221}^{33} + y_{222}^{33}) \tag{B10}$$

$$l_{n0}^{33} = \frac{3}{4\pi\rho_0\xi} y_2^{\text{Shear}}(r_s; n) = \left(\frac{r_s}{a}\right)^{n-2} (n y_{320}^{33} + y_{321}^{33}) \tag{B11}$$

$$k_{n0}^{33} = G a y_2^{\text{Tide}}(r_s; n) = n\left(\frac{r_s}{a}\right)^{n-2} y_{120}^{33} \tag{B12}$$

with constants:

$$y_{230}^{12} = -\frac{1}{16\pi\rho_0\beta^2}\frac{\mu_s d_s}{r_s}\left[-2 + \frac{d_s}{a}(P - Q)\right] \tag{B13}$$

$$y_{231}^{12} = -\frac{a}{16\pi\rho_0\beta^2}\frac{\mu_s}{r_s}\left[2M + \frac{d_s}{a}\left(2\frac{\alpha t}{\beta} - 3\Lambda - 2\Delta\mu\right)\right] \tag{B14}$$

$$y_{232}^{12} = -\frac{a}{16\pi\rho_0\beta^2}\frac{\mu_s}{r_s}\left[1 + \frac{1}{N}(2T + S - 6) + \Delta\mu\right] \tag{B15}$$

$$y_{330}^{12} = \frac{1}{16\pi\rho_0\beta^2}\frac{\mu_s d_s}{r_s}\left[-2 + \frac{d_s}{a}(P - Q)\right] \tag{B16}$$

$$y_{331}^{12} = \frac{a}{16\pi\rho_0\beta^2}\frac{\mu_s}{r_s}\left[\frac{2}{N} - \frac{d_s}{a}(1 + 6M)\right] \tag{B17}$$

$$y_{332}^{12} = \frac{a}{16\pi\rho_0\beta^2}\frac{\mu_s}{r_s}\left[-4\Lambda + \frac{2T + S}{N} + \Delta\mu\right] \tag{B18}$$

$$y_{130}^{12} = \frac{Ga}{4\beta^2}\frac{\mu_s d_s}{r_s}\left(1 - \frac{d_s}{2a}P\right) \tag{B19}$$

$$y_{131}^{12} = \frac{Ga}{4\beta^2}\frac{\mu_s d_s}{r_s}\left(1 - \frac{\alpha t}{\beta} + \Delta\nu\right) \tag{B20}$$

$$y_{132}^{12} = \frac{Ga^2}{8\beta^2}\frac{\mu_s}{r_s}(4 - T - \Delta\nu) \tag{B21}$$

$$y_{240}^{23} = -\frac{1}{8\pi a} d_s\left[-2 + \frac{d_s}{a}(P - Q + 2\Delta\mu)\right] \tag{B22}$$

$$y_{241}^{23} = -\frac{1}{8\pi a} d_s\left[1 - 2(P - Q + M + 2\Delta\mu) + \frac{2\alpha t}{\beta}(1 - M)\right] \tag{B23}$$

$$y_{340}^{23} = \frac{1}{8\pi a} d_s\left[-2 + \frac{d_s}{a}(P - Q + 2\Delta\mu)\right] \tag{B24}$$

$$y_{341}^{23} = \frac{1}{8\pi}\left[2 + \frac{d_s}{a}(3 - 2T - 2S - 2N\Delta\mu)\right] \tag{B25}$$

$$y_{342}^{23} = -\frac{1}{8\pi} \tag{B26}$$

$$y_{140}^{23} = \frac{1}{2} G\rho_0 d_s\left[1 - \frac{d_s}{2a}(P + 2\Delta\mu)\right] \tag{B27}$$

$$y_{141}^{23} = \frac{G\rho_0 N}{4} d_s\left(\Delta\nu - \frac{2\alpha t}{\beta}\right) \tag{B28}$$

$$y_{210}^{22} = -\frac{3}{4\pi\rho_0\beta^2}\frac{K_s\mu_s d_s}{\sigma_s r_s}\left[-2 + \frac{d_s}{a}(P - Q)\right] \tag{B29}$$

$$y_{211}^{22} = -\frac{3a}{4\pi\rho_0\beta^2}\frac{K_s\mu_s}{\sigma_s r_s}\left\{-\frac{2}{N} + \frac{2\alpha t}{\beta}\frac{d_s}{a}(2 - \Lambda) + \frac{d_s}{a} \times [\Lambda - S - 2\Delta\mu(N + 1)]\right\} \tag{B30}$$

$$y_{212}^{22} = -\frac{3a}{4\pi\rho_0\beta^2}\frac{K_s\mu_s}{\sigma_s r_s} \times \left[-\frac{S}{N} - 3\Delta\mu + \frac{2\alpha t}{\beta N}(2 - \Lambda) + 2M^2\left(\frac{\alpha t}{\beta} - 1\right)\right] \tag{B31}$$

$$y_{220}^{22} = -\frac{\lambda_s}{\sigma_s}\frac{d_s}{4\pi r_s}\left[-2 + \frac{d_s}{a}(P - Q + 2\Delta\mu)\right] \tag{B32}$$

$$y_{221}^{22} = -\frac{\lambda_s}{\sigma_s}\frac{a}{4\pi r_s}\left[-2 + \frac{d_s}{a}(5 - 2T)\right] \tag{B33}$$

$$y_{222}^{22} = \frac{\lambda_s}{\sigma_s}\frac{a}{4\pi r_s} \tag{B34}$$

$$y_{230}^{22} = \frac{3}{8\pi\rho_0\beta^2}\frac{K_s\mu_s d_s}{\sigma_s r_s}\left[-2 + \frac{d_s}{a}(P - Q)\right] \tag{B35}$$

$$y_{231}^{22} = \frac{3a}{8\pi\rho_0\beta^2}\frac{K_s\mu_s}{\sigma_s r_s}\left[2M + \frac{d_s}{a}\left(\frac{2\alpha t}{\beta} - 3\Lambda - 2\Delta\mu\right)\right] \tag{B36}$$

$$y_{232}^{22} = \frac{3a}{8\pi\rho_0\beta^2}\frac{K_s\mu_s}{\sigma_s r_s}\left[1 + \Delta\mu + \frac{1}{N}(2T + S - 6)\right] \tag{B37}$$

$$y_{310}^{22} = \frac{3a}{4\pi\rho_0\beta^2}\frac{K_s\mu_s d_s}{\sigma_s r_s}\left[-2 + \frac{d_s}{a}(P - Q)\right] \tag{B38}$$

$$y_{311}^{22} = \frac{3a^2}{4\pi\rho_0\beta^2}\frac{K_s\mu_s}{\sigma_s r_s} \times \left[-2M + \frac{d_s}{a}\left(1 + \frac{6}{N}\right) - \frac{2d_s}{a}(P - Q - 1 + 2T + 2\Delta\mu)\right] \tag{B39}$$

$$y_{312}^{22} = \frac{3a^2}{4\pi\rho_0\beta^2}\frac{K_s\mu_s}{\sigma_s r_s} \times \left[-1 + \frac{6}{N} - \frac{1}{N}(P - Q - 1 + 2T + 2\Delta\mu)\right] \tag{B40}$$

$$y_{320}^{22} = \frac{\lambda_s}{\sigma_s}\frac{d_s}{4\pi r_s}\left[-2 + \frac{d_s}{a}(P - Q + 2\Delta\mu)\right] \tag{B41}$$

$$y_{321}^{22} = \frac{\lambda_s}{\sigma_s}\frac{d_s}{4\pi r_s}\left[5 - 2M - \frac{2\alpha t}{\beta N}\right] \tag{B42}$$

$$y_{330}^{22} = -\frac{3}{8\pi\rho_0\beta^2}\frac{K_s\mu_s d_s}{\sigma_s r_s}\left[-2 + \frac{d_s}{a}(P - Q)\right] \tag{B43}$$

$$y_{331}^{22} = -\frac{3a}{8\pi\rho_0\beta^2}\frac{K_s\mu_s}{\sigma_s r_s}\left[\frac{2}{N} - \frac{d_s}{a}(1 + 6M)\right] \tag{B44}$$

$$y_{332}^{22} = -\frac{3a}{8\pi\rho_0\beta^2}\frac{K_s\mu_s}{\sigma_s r_s}\left[-4\Lambda + \frac{2T + S}{N} + \Delta\mu\right] \tag{B45}$$

$$y_{110}^{22} = \frac{3G}{2\beta^2}\frac{K_s\mu_s d_s}{\sigma_s r_s}(2a - d_s P) \tag{B46}$$

$$y_{111}^{22} = \frac{3Ga}{2\beta^2}\frac{K_s\mu_s}{\sigma_s r_s}\left[2a + d_s\left(2P - 4 - \frac{2\alpha t}{\beta} + 6\nu\right)\right] \tag{B47}$$

$$y_{112}^{22} = \frac{3Ga^2}{2\beta^2}\frac{K_s\mu_s}{\sigma_s r_s}\left[-2 + T - \frac{2\alpha t}{\beta} + 3\nu\right] \tag{B48}$$

$$y_{120}^{22} = \frac{\lambda_s}{\sigma_s} G\rho_0 d_s\left[1 - \frac{d_s}{2a}(P + 2\Delta\mu)\right] \tag{B49}$$

$$y_{130}^{22} = -\frac{3Ga}{2\beta^2}\frac{K_s\mu_s d_s}{\sigma_s r_s}\left(1 - \frac{d_s}{2a}P\right) \tag{B50}$$

$$y_{131}^{22} = -\frac{3Ga}{2\beta^2}\frac{K_s\mu_s d_s}{\sigma_s r_s}\left(1 - \frac{\alpha t}{\beta} + \Delta\nu\right) \tag{B51}$$

$$y_{132}^{22} = -\frac{3Ga^2}{4\beta^2}\frac{K_s\mu_s}{\sigma_s r_s}(4 - T - \Delta\nu) \tag{B52}$$

$$y_{220}^{33} = -\frac{1}{4\pi a}d_s\left[-2 + \frac{d_s}{a}(P - Q + 2\Delta\mu)\right] \tag{B53}$$

$$y_{221}^{33} = -\frac{1}{4\pi}\left[-2 + \frac{d_s}{a}(5 - 2T)\right] \tag{B54}$$

$$y_{222}^{33} = \frac{1}{4\pi} \tag{B55}$$

$$y_{320}^{33} = \frac{1}{4\pi a}d_s\left[-2 + \frac{d_s}{a}(P - Q + 2\Delta\mu)\right] \tag{B56}$$

$$y_{321}^{33} = \frac{1}{4\pi a}d_s\left(5 - 2M - \frac{2\alpha t}{\beta N}\right) \tag{B57}$$

$$y_{120}^{33} = G\rho_0 d_s\left[1 - \frac{d_s}{2a}(P + 2\Delta\mu)\right] \tag{B58}$$

where

α = P-wave velocity

β = S-wave velocity

ρ_0 = density at the surface

λ_s, μ_s = Lamé's constants at the source

d_s = source depth

G = Newton's gravitational constant

$$N = 1 - \frac{\beta^2}{\alpha^2}$$

$$M = \frac{\beta^2}{\alpha^2 - \beta^2}$$

$$\Lambda = \frac{\alpha^2 + \beta^2}{\alpha^2 - \beta^2}$$

$$\gamma = \tfrac{4}{3}\pi G\rho_0$$

$$t = \frac{g_0 a}{2\alpha\beta}$$

$$T = \frac{1 + \dfrac{\beta t}{\alpha}}{1 - \dfrac{\beta^2}{\alpha^2}}$$

$$\Delta\mu = \left.\frac{a}{\mu}\frac{d\mu}{dr}\right|_{r=a}$$

$$\Delta\rho_0 = \left.\frac{a}{\rho_0}\frac{d\rho}{dr}\right|_{r=a}$$

$$\Delta\nu = \Delta\mu - \frac{\Delta\rho_0}{2}$$

$$P = 1 + \frac{\beta t}{\alpha} - \left(1 + \frac{\beta^2}{\alpha^2}\right)\Delta\nu$$

$$S = \left.\frac{\beta^2}{\alpha^2}\frac{a}{\lambda + \mu}\frac{d(\lambda + \mu)}{dr}\right|_{r=a}$$

$$Q = \frac{\beta t}{\alpha} - S + \left(1 + \frac{\beta^2}{\alpha^2}\right)\frac{\Delta\rho_0}{2}$$

$$\xi = \frac{g_0}{\gamma a}$$

$$\sigma = \lambda + 2\mu$$

$$K = \lambda + \tfrac{2}{3}\mu.$$

C INFINITE SUMS OF LEGENDRE FUNCTIONS

We begin with the generating function of Legendre's polynomials,

$$F(r, \theta) \equiv \sum_{n=0}^{\infty} r^n P_n(\cos\theta) = \frac{1}{\sqrt{1 - 2r\cos\theta + r^2}} \tag{C1}$$

Integrating (C1) with respect to r gives the desired formulae.

$$\int_0^t \frac{F(r, \theta) - 1}{r}dr = \sum_{n=1}^{\infty}\frac{1}{n}t^n P_n(\cos\theta) = -\ln(1 - t\cos\theta + \sqrt{1 - 2t\cos\theta + t^2}) + \ln 2 \tag{C2}$$

$$\int_0^t ds\int_0^s \frac{F(r, \theta) - 1}{r}dr = \sum_{n=0}^{\infty}\frac{1}{n(n+1)}t^{n+1}P_n(\cos\theta) = -t\ln(1 - t\cos\theta + \sqrt{1 - 2t\cos\theta + t^2}) - \ln(t - \cos\theta + \sqrt{1 - 2t\cos\theta + t^2}) + \ln(1 - \cos\theta) + t\ln 2 \tag{C3}$$

$$\int_0^t ds\int_0^s dx\int_0^x \frac{F(r, \theta) - r\cos\theta - 1}{r^2}dr = \sum_{n=2}^{\infty}\frac{1}{n(n^2-1)}t^{n+1}P_n(\cos\theta) = (1 - \tfrac{1}{2}t\cos\theta)t\ln(1 - t\cos\theta + \sqrt{1 - 2t\cos\theta + t^2}) - t + \tfrac{1}{2}\ln(t - \cos\theta + \sqrt{1 - 2t\cos\theta + t^2}) - \tfrac{1}{2}\ln(1 - \cos\theta) + t(1 - \ln 2) + \tfrac{1}{2}t^2\cos\theta\ln 2 - \tfrac{1}{2}t\sqrt{1 - 2t\cos\theta + t^2} + \tfrac{1}{4}t^2\cos\theta. \tag{C4}$$

Differentiations of (C1) gives

$$\sum_{n=0}^{\infty} nt^{n-1}P_n(\cos\theta) = \frac{1}{(1 - 2t\cos\theta + t^2)^{3/2}}(\cos\theta - t). \tag{C5}$$

In the same way, we obtain the following formulae after some manipulations.

$$\sum_{n=0}^{\infty} n^2 t^{n-1}P_n(\cos\theta) = \frac{1}{(1 - 2t\cos\theta + t^2)^{5/2}}[(1 - t^2)\cos\theta + t(\cos^2\theta - 2 + t^2)] \tag{C6}$$

$$\sum_{n=0}^{\infty} n^3 t^{n-1} P_n(\cos\theta)$$
$$= \frac{1}{(1-2t\cos\theta+t^2)^{7/2}}[-t^5 - t^4\cos\theta + t^3(10-2\cos^2\theta) + t^2\cos\theta(\cos^2\theta-9) + t(5\cos^2\theta-4) + \cos\theta] \quad \text{(C7)}$$

$$\sum_{n=0}^{\infty} n^4 t^{n-1} P_n(\cos\theta)$$
$$= \frac{1}{(1-2t\cos\theta+t^2)^{9/2}}[t^7 + 7t^6\cos\theta + t^5(9\cos^2\theta-36) + t^4\cos\theta(21-2\cos^2\theta) + t^3(\cos^4\theta - 42\cos^2\theta + 60) + t^2\cos\theta(18\cos^2\theta-45) + t(15\cos^2\theta-8) + \cos\theta] \quad \text{(C8)}$$

$$\sum_{n=0}^{\infty} (n+1) t^{n-1} P_n(\cos\theta) = \frac{1-t\cos\theta}{t(1-2t\cos\theta+t^2)^{3/2}} \quad \text{(C9)}$$

$$\sum_{n=0}^{\infty} n(n+1) t^{n-1} P_n(\cos\theta)$$
$$= \frac{1}{(1-2t\cos\theta+t^2)^{5/2}} \times [2\cos\theta - t(3+\cos^2\theta-2t\cos\theta)] \quad \text{(C10)}$$

$$\sum_{n=2}^{\infty} \frac{1}{n-1} t^{n-1} P_n(\cos\theta)$$
$$= \frac{1}{t}\sqrt{1-2t\cos\theta+t^2} - \cos\theta\ln\left(1-t\cos\theta + \sqrt{1-2t\cos\theta+t^2}\right) - \cos\theta(1-\ln 2) \quad \text{(C11)}$$

$$\sum_{n=0}^{\infty} \frac{1}{n+1} t^{n+1} P_n(\cos\theta)$$
$$= \ln(t - \cos\theta + \sqrt{1-2t\cos\theta+t^2}) - \ln(1-\cos\theta) \quad \text{(C12)}$$

$$\sum_{n=2}^{\infty} \frac{n}{n-1} t^{n-1} P_n(\cos\theta)$$
$$= -\frac{1}{t} - \cos\theta[2 - \ln 2 + \ln(1 - t\cos\theta + \sqrt{1-2t\cos\theta+t^2})] + \frac{2+t(t-2\cos\theta)}{t\sqrt{1-2t\cos\theta+t^2}} \quad \text{(C13)}$$

$$\sum_{n=0}^{\infty} t^n \frac{\partial P_n(\cos\theta)}{\partial\theta} = -\frac{t\sin\theta}{(1-2t\cos\theta+t^2)^{3/2}} \quad \text{(C14)}$$

$$\sum_{n=0}^{\infty} n t^{n-1} \frac{\partial P_n(\cos\theta)}{\partial\theta} = -\frac{\sin\theta(1+t\cos\theta-2t^2)}{(1-2t\cos\theta+t^2)^{5/2}} \quad \text{(C15)}$$

$$\sum_{n=0}^{\infty} n^2 t^{n-1} \frac{\partial P_n(\cos\theta)}{\partial\theta}$$
$$= -\frac{\sin\theta}{(1-2t\cos\theta+t^2)^{7/2}} \times [1 + 5t\cos\theta + t^2(\cos^2\theta - 10) - t^3\cos\theta + 4t^4] \quad \text{(C16)}$$

$$\sum_{n=1}^{\infty} \frac{1}{n} t^n \frac{\partial P_n\cos\theta)}{\partial\theta} = -\frac{\cos\theta}{\sin\theta} - \frac{t-\cos\theta}{\sin\theta\sqrt{1-2t\cos\theta+t^2}} \quad \text{(C17)}$$

$$\sum_{n=1}^{\infty} \frac{1}{n(n+1)} t^{n+1} \frac{\partial P_n(\cos\theta)}{\partial\theta}$$
$$= \frac{1}{\sin\theta}(1 - t\cos\theta - \sqrt{1-2t\cos\theta+t^2}) \quad \text{(C18)}$$

$$\sum_{n=2}^{\infty} \frac{1}{n(n^2-1)} t^{n+1} \frac{\partial P_n(\cos\theta)}{\partial\theta}$$
$$= \frac{1}{2\sin\theta}[t\cos\theta(2-t\cos\theta) - 1] + \frac{1}{2\sin\theta\sqrt{1-2t\cos\theta+t^2}} \times [1 + 2t^2 + t\cos\theta(t\cos\theta - 3 - t^2)] + \tfrac{1}{2}t^2\sin\theta \cdot \left[\ln\frac{1}{2}(1 - t\cos\theta + \sqrt{1-2t\cos\theta+t^2}) - \frac{1}{\sqrt{1-2t\cos\theta+t^2}} - \frac{1}{2}\right] \quad \text{(C19)}$$

$$\sum_{n=2}^{\infty} \frac{1}{n-1} t^{n-1} \frac{\partial P_n(\cos\theta)}{\partial\theta}$$
$$= \frac{1-t\cos\theta}{\sin\theta\sqrt{1-2t\cos\theta+t^2}} + \sin\theta\ln(1 - t\cos\theta + \sqrt{1-2t\cos\theta+t^2}) - \frac{\cos^2\theta}{\sin\theta} + \sin\theta(1-\ln 2) \quad \text{(C20)}$$

$$\sum_{n=0}^{\infty} \frac{1}{n+1} t^{n+1} \frac{\partial P_n(\cos\theta)}{\partial\theta}$$
$$= -\frac{1}{\sin\theta} + \frac{1-t\cos\theta}{\sin\theta\sqrt{1-2t\cos\theta+t^2}} \quad \text{(C21)}$$

$$\sum_{n=2}^{\infty} t^{n-1} P_n^2(\cos\theta) = \frac{3t\sin^2\theta}{(1-2t\cos\theta+t^2)^{5/2}} \quad \text{(C22)}$$

$$\sum_{n=2}^{\infty} \frac{1}{n} t^{n-1} P_n^2(\cos\theta)$$
$$= \frac{1}{t}\left[\frac{2}{\sin^2\theta} - 1 - \frac{1-t\cos\theta}{(1-2\cos^2\theta+t^2)^{3/2}} + \frac{2\cos\theta(t-\cos\theta)}{\sin^2\theta\sqrt{1-2\cos^2\theta+t^2}}\right] \quad \text{(C23)}$$

$$\sum_{n=2}^{\infty} \frac{1}{n(n+1)} t^{n-1} P_n^2(\cos\theta)$$
$$= \frac{1}{t}\left[1 - \frac{1}{\sqrt{1-2t\cos\theta+t^2}} - \frac{2\cos\theta}{t\sin^2\theta}(1 - t\cos\theta - \sqrt{1-2t\cos\theta+t^2})\right] \quad \text{(C24)}$$

$$\sum_{n=2}^{\infty} \frac{1}{n(n^2-1)} t^{n-1} P_n^2(\cos\theta)$$
$$= \tfrac{1}{2}\cos\theta + \frac{\cos\theta}{t^2\sin^2\theta}(1-2t\cos\theta+t^2) - \frac{1}{t^2\sin^2\theta\sqrt{1-2t\cos\theta+t^2}} \times [\cos\theta + t^3(1-2\cos^2\theta) + t(1-t\cos\theta)(1-4\cos^2\theta)] \quad \text{(C25)}$$

$$\sum_{n=2}^{\infty}\frac{1}{n+1}t^{n-1}P_n^2(\cos\theta)$$
$$=-\frac{2\cos\theta}{t^2\sin^2\theta}\left(-1+\frac{1-t\cos\theta}{\sqrt{1-2t\cos\theta+t^2}}\right)$$
$$-\frac{\cos\theta-t}{(1-2\cos^2\theta+t^2)^{3/2}} \tag{C26}$$

$$\sum_{n=2}^{\infty}\frac{1}{n-1}t^{n-1}P_n^2(\cos\theta)$$
$$=\cos\theta\left(1+\frac{2}{\sin^2\theta}\right)+\frac{2}{t}(1-\sqrt{1-2t\cos\theta+t^2})$$
$$+\frac{t-\cos\theta}{(1-2\cos^2\theta+t^2)^{3/2}}$$
$$-\frac{2}{\sqrt{1-2\cos^2\theta+t^2}}\cdot\left[\frac{1}{t}+\frac{\cos\theta}{\sin^2\theta}(1-t\cos\theta)\right] \tag{C27}$$

$$\sum_{n=2}^{\infty}\frac{1}{n^2-1}t^{n-1}P_n^2(\cos\theta)$$
$$=\frac{1}{2t^2\sin^2\theta}[2(t\sin^2\theta-\cos\theta)+t^2\cos\theta(2+\sin^2\theta)]$$
$$-\sqrt{1-2t\cos\theta+t^2}+\frac{1}{t^2\sin^2\theta\sqrt{1-2t\cos\theta+t^2}}$$
$$\times(\cos\theta-t-t^2\cos\theta+t^3\cos^2\theta). \tag{C28}$$